

**UNCLASSIFIED**

---

---

**AD 268 504**

*Reproduced  
by the*

**ARMED SERVICES TECHNICAL INFORMATION AGENCY  
ARLINGTON HALL STATION  
ARLINGTON 12, VIRGINIA**



---

---

**UNCLASSIFIED**

**NOTICE:** When government or other drawings, specifications or other data are used for any purpose other than in connection with a definitely related government procurement operation, the U. S. Government thereby incurs no responsibility, nor any obligation whatsoever; and the fact that the Government may have formulated, furnished, or in any way supplied the said drawings, specifications, or other data is not to be regarded by implication or otherwise as in any manner licensing the holder or any other person or corporation, or conveying any rights or permission to manufacture, use or sell any patented invention that may in any way be related thereto.

**268504**  
CATALOGED BY ASTIA  
AS AD NO.

~~SELENIA~~ S.p.A.

MONITORING AGENCY DOCUMENT NR. **AFCRL-981**

XEROX

62-1-5

195 850

ASTIA DOCUMENT NR.

"PROPAGATION CHARACTERISTICS OF A MAGNETO-IONIC DUCT"

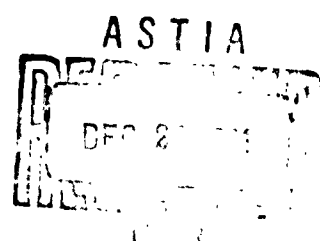
Ing. D. Formato & Ing. A. Gilardini

SELENIA S.p.A., Via Tiburtina Km. 12,400, ROME, ITALY

TECHNICAL (SCIENTIFIC) NOTE NO. 2

CONTRACT NO. AF 61 (052) - 145

May 1, 1961



**268504**

The research reported in this document has been sponsored by the Air Force Cambridge Research Center of the Air Research and Development Command, United States Air Force, through its European Office.

Abstract

The propagation characteristics of a uniform magneto-ionic duct of circular cross-section are determined for frequencies higher than the cyclotron frequency. The ratios (plasma wavelength) / (free space wavelength) and (power flowing in the plasma) / (power flowing outside) are evaluated and discussed as a function of the diameter / wavelength ratio and of the plasma permittivity for the propagation of circularly symmetrical modes.

The Brillouin diagrams for frequencies higher and lower than the cyclotron frequency are also derived.

Table of contents

Introduction	pag
Summary of the previous results	"
Propagation in the $0 < \epsilon_i < 1$ , $\epsilon_i < \epsilon_3 < 1$ region	"
Propagation in the $-\infty < \epsilon_i < 0$ , $0 < \epsilon_3 < 1$ region	"
Propagation in the $-\infty < \epsilon_i < 0$ , $\epsilon_i < \epsilon_3 < 0$ region	"
Brillouin diagrams	"
Bibliography	"

### Introduction

In Technical Note N.1 we have investigated electro-magnetic wave propagation in a magneto-ionic duct, namely in a cylindrical plasma of circular cross-section in a static axial magnetic field, assuming signal frequencies lower than the cyclotron frequency.

In this Note the same general analysis is extended to the case of signal frequencies higher than the cyclotron frequency. Here too the discussion is based on the general characteristic equation and restricted to a uniform, non-attenuating plasma and to circularly symmetrical modes; the permittivity tensor is chosen as a constant parameter for each solution. From these and the previous results we have derived the Brillouin diagrams relating the guided and the free space phase constants for a given set of plasma frequency and cyclotron frequency values. These diagrams are similar to those derived with the so-called quasi-static approximation, except for a few special features, which will be described.

1) Summary of the previous results

The dielectric constant of a uniform plasma, in the absence of agitational or drift motion, placed in a steady-state magnetic field  $\mathbf{B}$  directed along the positive  $z$ ( $i, l = 3$ ) axis, is a tensor  $||\epsilon||$  defined by the formula:

$$D_i = \epsilon_{ii} E_i$$

where

$$\begin{aligned}\epsilon_{11} &= \epsilon_{zz} = \epsilon_0 \epsilon_1 = \epsilon_0 \left( 1 + \frac{\omega_p^2}{\omega_b^2 - \omega^2} \right) \\ \epsilon_{33} &= \epsilon_0 \epsilon_3 = \epsilon_0 \left( 1 - \frac{\omega_p^2}{\omega^2} \right) \\ \epsilon_{12} &= -\epsilon_{21} = j \epsilon_0 \epsilon_2 = j \epsilon_0 \frac{\omega_b}{\omega} \cdot \frac{\omega_p^2}{\omega_b^2 - \omega^2}\end{aligned}\quad (1)$$

$$\omega_p^2 = \frac{n e^2}{m \epsilon_0}$$

$$\omega_b = \frac{e B}{m}$$

$n$  = electron density

$m$  = electron mass

$e$  = electron charge

From the equations(1), one can easily find the following relation among  $\epsilon_1$ ,  $\epsilon_2$  and  $\epsilon_3$

$$\epsilon_0^2 = (\epsilon_1 - 1)(\epsilon_1 - \epsilon_3) \quad (2)$$

If the plasma is uniform and in steady state conditions and we take a system of cylindrical orthogonal coordinates  $r, \varphi, z$  where the  $z$  axis is parallel to  $\mathbf{B}$  and with the same orientation, the Maxwell equations can be solved and the field equations for the circularly symmetrical modes written :

inside the plasma:

$$E_z = A_1 J_0(x_1 s/R) + A_2 J_0(x_2 s/R)$$

$$E_p = -j \frac{2\pi R}{\lambda_0} \left\{ \frac{\epsilon_s}{\epsilon_i} \left[ A_1 \frac{s_1}{x_1} J_1(x_1 s/R) + A_2 \frac{s_2}{x_2} J_1(x_2 s/R) \right] + \frac{\epsilon_s}{\epsilon_i} \alpha \left[ A_1 \frac{1}{x_1} J_1(x_1 p/R) + A_2 \frac{1}{x_2} J_1(x_2 p/R) \right] \right\}$$

$$E_p = \frac{2\pi R}{\lambda_0} \left[ A_1 \frac{s_1}{x_1} J_1(x_1 s/R) + A_2 \frac{s_2}{x_2} J_1(x_2 s/R) \right] \quad (3)$$

$$H_p = -\frac{2\pi R}{\lambda_0} \frac{\alpha}{Z_0} \left[ A_1 \frac{s_1}{x_1} J_1(x_1 p/R) + A_2 \frac{s_2}{x_2} J_1(x_2 p/R) \right]$$

$$H_\varphi = j \frac{2\pi R}{\lambda_0} \frac{\epsilon_s}{Z_0} \left[ A_1 \frac{1}{x_1} J_1(x_1 p/R) + A_2 \frac{1}{x_2} J_1(x_2 p/R) \right]$$

$$H_z = j \frac{1}{Z_0} \left[ A_1 s_1 J_0(x_1 p/R) + A_2 s_2 J_0(x_2 p/R) \right]$$

outside the plasma:

$$E_z = B K_0(x_0 p/R)$$

$$E_p = -j \frac{2\pi R}{\lambda_0} \alpha B \frac{1}{x_0} K_1(x_0 p/R)$$

$$E_\varphi = -\frac{2\pi R}{\lambda_0} C \frac{1}{x_0} K_1(x_0 p/R) \quad (4)$$

$$H_p = \frac{2\pi R}{\lambda_0} \frac{\alpha}{Z_0} C \frac{1}{x_0} K_1(x_0 p/R)$$

$$H_\varphi = -j \frac{2\pi R}{\lambda_0} \frac{1}{Z_0} B \frac{1}{x_0} K_1(x_0 p/R)$$

$$H_z = j \frac{1}{Z_0} \cdot C \cdot K_0(x_0 p/R)$$

where:

$R = \frac{d}{2}$  = radius of the plasma cylinder

$\alpha = \frac{\lambda_0}{\lambda_g}$  = free space to guided wavelength ratio ( $> 1$ )

$Z_0 = \sqrt{\mu_0 / \epsilon_0}$  = free space characteristic impedance

Moreover:

$$x_{1,2} = \frac{2\pi R}{\lambda_0} \delta_{1,2} (\alpha^2 - 1)^{\frac{1}{2}} = \delta_{1,2} x_0 \quad (5)$$

$$x_0 = \frac{2\pi R}{\lambda_0} (\alpha^2 - 1)^{\frac{1}{2}}$$

and

$$\delta_{1,2}^2 = \frac{\epsilon_3(\epsilon_1 - \alpha^2)}{\epsilon_1(\alpha^2 - 1)} + \frac{\epsilon_1 - \epsilon_3}{2\epsilon_1} \left[ -1 \pm \sqrt{1 + 4 \frac{\epsilon_3(\epsilon_1 - 1)}{\epsilon_1 - \epsilon_3} \cdot \frac{\alpha^2}{(\alpha^2 - 1)^2}} \right] \quad (6)$$

$$g_{1,2} = \frac{\epsilon_1 \delta_{1,2}^2 (\alpha^2 - 1) - \epsilon_3 (\epsilon_1 - \alpha^2)}{\alpha \epsilon_2}$$

If the boundary conditions are imposed, the following equations result:

$$\begin{aligned} \frac{B}{A_1} &= \frac{J_0(x_1) + \frac{A_2}{A_1} J_0(x_2)}{K_0(x_0)} \\ \frac{C}{A_1} &= \frac{g_1 J_0(x_1) + g_2 \frac{A_2}{A_1} J_0(x_2)}{K_0(x_0)} \\ \frac{A_1}{A_1} &= - \frac{g_1}{g_2} \frac{\frac{1}{\delta_1} J_1(x_1) + \frac{K_1(x_0)}{K_0(x_0)} J_0(x_1)}{\frac{1}{\delta_2} J_1(x_2) + \frac{K_1(x_0)}{K_0(x_0)} J_0(x_2)} \\ \frac{A_2}{A_1} &= - \frac{\frac{\epsilon_3}{\delta_1} J_1(x_1) + \frac{K_0(x_0)}{K_0(x_0)} J_0(x_1)}{\frac{\epsilon_3}{\delta_2} J_1(x_2) + \frac{K_1(x_0)}{K_0(x_0)} J_0(x_2)} \end{aligned}$$

The last two equations are consistent only if

$$F(x_0, \delta_1, \epsilon_3) = \gamma F(x_0, \delta_2, \epsilon_3) \quad (7)$$

where

$$F(x_0, S, \epsilon_3) = \frac{\frac{1}{\delta} \frac{J_1(Sx_0)}{J_0(Sx_0)} + \frac{K_1(x_0)}{K_0(x_0)}}{\frac{\epsilon_3}{\delta} \frac{J_1(Sx_0)}{J_0(Sx_0)} + \frac{K_1(x_0)}{K_0(x_0)}} \quad (8)$$

$$\gamma = \frac{g_1}{g_2} = \frac{1 - \sqrt{1 + 4\epsilon_3(\epsilon_1-1)\alpha^2}/(\epsilon_1-\epsilon_3)(\alpha^2-1)^2}{1 + \sqrt{1 + 4\epsilon_3(\epsilon_1-1)\alpha^2}/(\epsilon_1-\epsilon_3)(\alpha^2-1)^2}$$

For each assumed set of  $\alpha$ ,  $\epsilon_1$  and  $\epsilon_3$  values, the variable  $x_0$  is the only unknown in (7) and it can be determined.

The  $d/\lambda_0$  value which corresponds to the assumed  $\alpha$ ,  $\epsilon_1$  and  $\epsilon_3$  set is then computed from the equation:

$$d/\lambda_0 = x_0 / \pi \sqrt{(\alpha^2-1)}$$

when  $\epsilon_3 < 0$  and  $\alpha^2$  is smaller than

$$\alpha_i^2 = (\epsilon_1 - \epsilon_3)^{-1} \cdot [\epsilon_1 + \epsilon_3 - 2\epsilon_1\epsilon_3 + 2\sqrt{\epsilon_1\epsilon_3(\epsilon_1-1)(\epsilon_3-1)}]$$

the quantities  $\delta_{1,2}^2$  are complex.

In this case we write:

$$\delta_{1,2}^2 = |\delta|^2 \exp(\pm \epsilon j\theta)$$

$$g_{1,2} = |\delta| \exp(\pm j\vartheta)$$

$$J_0(\delta_{1,2} x_0) = S_0(|\delta| x_0, \theta) \exp[\pm j \psi_0(|\delta| x_0, \theta)]$$

$$J_1(\delta_{1,2} x_0) = S'_1(|\delta| x_0, \theta) \exp[\pm j \psi_1(|\delta| x_0, \theta)]$$

so that equation (7) can be written as an equation of only real quantities as follows:

$$\frac{\epsilon_3}{\delta^2} \cdot \frac{S_i^2}{S_o^2} + \frac{K_i^2(x_0)}{K_o^2(x_0)} = \quad (9)$$

$$= - \frac{1}{\delta} \frac{S_i}{S_o} \frac{K_i(x_0)}{K_o(x_0)} \left[ \frac{\epsilon_3 \sin[(\vartheta + \theta) - (\psi_i - \psi_o)]}{\sin \vartheta} + \frac{\sin[(\vartheta - \theta) + (\psi_i - \psi_o)]}{\sin \vartheta} \right]$$

The parameter  $x_0$  can thus be computed solving this last equation.

It is convenient to divide the entire range of  $\epsilon_i$  and  $\epsilon_3$  values, which may exist according to eqs. (1), into four regions:

1)  $1 < \epsilon_i < +\infty$   
 $-\infty < \epsilon_3 < 1$

2)  $0 < \epsilon_i < 1$   
 $\epsilon_i < \epsilon_3 < 1$

3)  $-\omega < \epsilon_i < 0$   
 $0 < \epsilon_3 < 1$

4)  $-\infty < \epsilon_i < 0$   
 $\epsilon_i < \epsilon_3 < 0$

The first region was examined in the Technical Scientific Note N. 1. All the other three regions satisfy the condition  $\omega > \omega_b$  and are examined here.

2) Propagation in the  $0 < \epsilon_1 < 1$ ,  $\epsilon_1 < \epsilon_3 < 1$  region

In this region the angular frequency is higher than  $\omega_c$ .

$$\omega_c = \sqrt{\omega_p^2 + \omega_b^2}$$

A simple discussion of eqs. (6) and (8) shows that  $\delta_{1,2}^2$  and  $\gamma^2$  are always negative for  $1 < \alpha^2 < \infty$ . Since  $\gamma F_1$  is then always negative and  $F_2$  positive (see fig. 1), no solution exists in this region. The conclusion is that  $\omega_c$  is a cut-off frequency and no propagation is possible for  $\omega > \omega_c$ .

3) Propagation in the  $-\infty < \epsilon_1 < 0$ ,  $0 < \epsilon_3 < 1$  region

Here  $\gamma^2$  and  $\delta_2^2$  are always negative (see fig. 2, 3) and  $\delta_1^2$  positive. The curves of fig. 1 are still valid in this case and show that an infinite set of solutions exists. In the frequency range this region corresponds to the conditions

$$\omega_b < \omega < \omega_c \quad \text{if } \omega_p < \omega_b \quad \text{and} \quad \omega_p < \omega < \omega_c \quad \text{if } \omega_p > \omega_b$$

When  $\alpha^2$  approaches unity,  $x_0$  tends to zero and  $d/\lambda_0$  to one of the values  $(d/\lambda_0)_c$ ,

$$(d/\lambda_0)_c = \frac{x_0^{(m)}}{\pi} \cdot \left[ \frac{\epsilon_1}{\epsilon_3(\epsilon_1-1) - \sqrt{\epsilon_3(\epsilon_1-1)(\epsilon_1-\epsilon_3)}} \right]^{\frac{1}{2}}$$

where  $x_0^{(m)}$  is the  $m^{\text{th}}$  root of  $J_0$ .

When  $\alpha^2$  approaches infinity,  $\gamma$  tends to zero and the solution tends to one of the  $x_0$  poles of  $F_2$ , namely to  $\gamma^{(m)}(\delta_\infty, \epsilon_3)$ , where  $\delta_\infty = -\epsilon_3/\epsilon_1$  and  $\gamma^{(m)}(\delta_\infty, \epsilon_3)$  is the  $m^{\text{th}}$  root of the equation

$$\frac{\epsilon_3}{\delta_\infty} \frac{J_1(\delta_\infty x_0)}{J_0(\delta_\infty x_0)} = - \frac{K_1(x_0)}{K_0(x_0)}$$

Consequently  $d/\lambda_0$  approaches zero.

The behaviour of  $X_0$  is shown in fig. 4 for the special case  $\epsilon_1 = -2$ ,  $\epsilon_3 = 0.5$ , while in fig. 5 and 6 we have plotted  $\lambda_g/\lambda_0$  and  $P_p/P_a$  versus  $d/\lambda_0$  ( $P_p$  and  $P_a$  being respectively the power flowing inside and outside the plasma).

The very unusual characteristics of this type of propagation are summarized below:

- 1) For each mode propagation can take place only for values of the  $d/\lambda_0$  ratio between zero and a maximum  $(d/\lambda_0)_m \geq (d/\lambda_0)_c$  which is characteristic of that mode.
- 2) For a given mode, when  $d/\lambda_0$  is between  $(d/\lambda_0)_c$  and  $(d/\lambda_0)_m$  propagation can take place with two different  $\lambda_g/\lambda_0$  ratios, but their group-velocities are opposite in sign.
- 3) The axial flows of electromagnetic power in the air and in the plasma have generally opposite directions. If  $P_p > P_a$  we have an "average" forward wave, if  $P_p < P_a$  an "average" backward wave. The points labeled "A" in fig. 5, where the group-velocity is zero, correspond to the points "A" in fig. 6 where  $P_p = P_a$ , so that although some power is really flowing separately in the air and in the plasma, the total average flow is zero.
- 4) The highest ratio  $P_p/P_a$  is obtained at  $d/\lambda_0=0$ ; at this point the  $m^{\text{th}}$  mode power ratio is:

$$\left(\frac{P_p}{P_a}\right)^{(m)}_{\max} = \frac{\epsilon_3 + \frac{2}{\lambda^{(m)}} \frac{K_1(\nu^{(m)})}{K_0(\nu^{(m)})} - \frac{1}{\epsilon_3} \frac{K_1^2(\nu^{(m)})}{K_0^2(\nu^{(m)})}}{1 - \frac{2}{\lambda^{(m)}} \frac{K_1(\nu^{(m)})}{K_0(\nu^{(m)})} - \frac{K_1^2(\nu^{(m)})}{K_0^2(\nu^{(m)})}}$$

#### 4) Propagation in the $-\infty < \epsilon_1 < 0$ , $\epsilon_1 < \epsilon_3 < 0$ region

Here in the  $\alpha_1^2 < \alpha^2 < \infty$  range  $\delta_{1,2}^2$  is are negative (fig. 7) and  $\tau'$  is positive and smaller than unity (fig. 8); the behaviour of  $F_{1,2}$  for the general case  $\epsilon_1 < 0$  is shown in fig. 9.

The curves indicate that in this region only one  $X_0$  solution may exist.

When  $\alpha$  approaches infinity,  $\gamma$  tends to zero and the  $X_0$  solution of the dispersion equation tends to  $v''(\sqrt{\epsilon_0}, \epsilon_3)$  if  $|\delta_{\omega}| < |\epsilon_3|$ . The parameter  $X_0$  increases when  $\alpha$  decreases and approaches infinity at  $\bar{\alpha}$ , the root of the equation:

$$\gamma \frac{1+|\delta_{\omega}|}{\epsilon_3 + |\delta_{\omega}|} = \frac{1+|\delta_{\omega}|}{\epsilon_3 + |\delta_{\omega}|} \quad \text{when } \bar{\alpha} > \alpha;$$

$$\frac{|\delta_{\omega}|^2 + \epsilon_3}{|\delta_{\omega}|} = \epsilon_3 \frac{\cos(\theta + \varphi)}{\sin \theta} - \frac{\cos(\theta - \varphi)}{\sin \theta} \quad \text{when } \bar{\alpha} < \alpha;$$

When  $\bar{\alpha} < \alpha$ , the  $X_0$  solution crosses continuously the  $\alpha$ ; abscissa and tends to infinity in the complex region.

Curves of  $|\delta_{\omega}|, \theta, \varphi$  are plotted in figs. 10 to 12 for the special case  $\epsilon_1 = -2$ ,  $\epsilon_3 = -1.5$ , while the  $X_0$  versus  $\alpha$  curve is given in fig. 13.

When  $|\delta_{\omega}| > |\epsilon_3|$  the curves show clearly that no solution exists at  $\alpha \rightarrow \infty$ ; then we do not expect any solution also at finite  $\alpha$  values. The propagation region is thus bounded by the condition  $\epsilon_1 \cdot \epsilon_3 \geq 1$  and becomes:

$$\left\{ \begin{array}{l} -\infty < \epsilon_1 < -1 \\ \epsilon_1 < \epsilon_3 < 1/\epsilon_1 \end{array} \right.$$

In the frequency domain this corresponds to the range:

$$\omega_b < \omega < \omega_c / \sqrt{2} < \omega_p$$

With the usual formulas the  $\lambda_g/\lambda_0$  and  $P_r/P_0$  versus  $d/\lambda_0$  curves can be calculated; they are plotted in figs. 14 and 15, for the case:  $\epsilon_1 = -2$ ;  $\epsilon_3 = -1.5$ .

We shall finally note that, as in the previous case, the power outside the plasma flows in a direction opposite

to that of power inside so that, being generally  $P_o \ll P_s$ , the power flow in the plasma is backward although the total power is flowing forward.

### BRILLOUIN DIAGRAMS

Keeping  $\epsilon_1$  and  $\epsilon_3$  as constant parameters in the Maxwell equations, it has been possible to solve the dispersion equation with a straightforward procedure. Brillouin diagrams ( $\beta = \frac{c\pi}{\lambda_g}$  versus  $\omega$ ) are, instead, more difficult to derive because  $\epsilon_1$  and  $\epsilon_3$  are functions of frequency.

In order to obtain from our computed data these diagrams, we have to solve the following system:

$$(10) \quad \begin{cases} \lambda_g/\lambda_0 = f(d/\lambda_0, \epsilon_1, \epsilon_3) \\ \epsilon_1 = \left( 1 + \frac{\omega_p^2}{\omega_b^2 - \omega^2} \right) \\ \epsilon_3 = \left( 1 - \frac{\omega_p^2}{\omega^2} \right) \end{cases}$$

Let us keep constant the ratio  $\alpha = \frac{\omega_p^2}{\omega_b^2}$  and choose all the pairs of  $\epsilon_1$  and  $\epsilon_3$  values which satisfy the equation:

$$(11) \quad \epsilon_1 = \frac{\alpha(1-\epsilon_3) - \epsilon_3}{\alpha(1-\epsilon_3) - 1} \quad (\text{see fig. 16})$$

The first two equations of the system (10) allows us to plot in the  $2\pi d/\lambda_0 = Kd$  versus  $2\pi d/\lambda_g = \beta d$  plane a set of curves,  $\epsilon_3$  being a constant for each curve. Let us find the intercepts of these curves:

$$(12) \quad Kd = f'(\beta d, \alpha, \epsilon_3)$$

With the straight lines:

$$(13) \quad K_d = K_p d / \sqrt{1 - \epsilon_s}$$

which represents the third equation of the above system (10),  $K_p d$  being the plasma density parameter  $\omega_p d/c$ .

For given values of the frequency independent parameters  $a$  and  $K_p d$ , these intercepts at different  $\epsilon_s$  values plotted in the  $K_d$  versus  $\beta d$  plane provide the Brillouin diagrams:

$$(14) \quad \beta d = F(K_d, a, K_p d)$$

The computation have been performed for two  $a$  values, the first being chosen in the  $\epsilon_s > 0$  region ( $a = 2.25$ ), the second in the  $\epsilon_s < 0$  region ( $a = 0.5$ ). In figs. 17 to 20 we have plotted the curves given by the equation (12) for the first  $X_0$  solutions and respectively for the conditions I)  $a = 2.25, \epsilon_s > 0$ ; II)  $a = 2.25, \epsilon_s < 0$ ; III)  $a = 0.5$ , IV)  $a = 0.5, \epsilon_s > 0$ .

The Brillouin diagrams, which result from these and similar curves for the second  $X_0$  solutions, are plotted in figs. 21 to 24. For each case three  $K_p d$  values have been considered, namely: 1.5, 3.5, 10.

It is interesting to compare these curves with the corresponding curves obtained by Could and Trivelpiece<sup>(3)</sup> and by Smulkin and Chorney<sup>(4)</sup> using the so-called quasi-static approximation. These authors have studied the more general case of a circular waveguide partially filled with plasma; from their results the curves to be used in our case are easily derived by setting the waveguide diameter equal to infinity.

No significant difference is found in the behaviour of the Brillouin diagrams in the  $\omega < \omega_p$  region ( $K_d < K_p d$ ).

In this region all the  $K_d$  versus  $\beta d$  curves start from the

origin and approach asymptotically the value  $K_p d$  or  $K_b d$ , whichever is smaller, except the first solution mode which, when  $\omega_p > \omega_b$ , approaches the asymptotic value  $(K_p^2 d^2 + K_b^2 d^2)^{1/2} / \sqrt{2}$ .

A behaviour, slightly more complicated than predicted from the quasi-static approximation, is found in the  $\omega > \omega_p$  region. Here the curves start from different points of the  $Kd = \beta d$  line between  $K_p d$  and  $\sqrt{K_p^2 d^2 + K_b^2 d^2}$  and approach the asymptotic value  $K_p d$  or  $K_b d$ , whichever is larger. The slopes of these curves may be positive, negative or partially positive and partially negative, so that the waves can be forward or backward. It is worth to note that in the quasi-static approximation all these waves are always backward.

The following details can be added to the discussed features in the  $\omega > \omega_p$  region. The Brillouin diagrams starting points on the  $Kd = \beta d$  line are given from the simple relation:

$$Kd = K_p d \frac{\sqrt{a + (1+c)^2}}{1+c}$$

where:  $c = K_p d / 2 \lambda_0^m$

Another simple relation can be found, which allows us to distinguish between forward and backward waves in the  $\omega_b > \omega_p$  region. Let us observe the behaviour of the intercepts which provide the Brillouin diagrams, when  $\epsilon_s$  increases from zero to unity and  $Kd$  varies consequently from  $K_p d$  to infinity. Fig. 17 indicates clearly that, when the intercept points fall in the positive  $\epsilon_s$  region, there is only one intercept for each  $\epsilon_s$  value. In this case the  $Kd$  versus  $\beta d$  curve has everywhere a positive slope, the limit  $\beta d \rightarrow \infty$  will be attained when  $Kd = K_b d$ , since it has to be considered as the intercept with the  $\epsilon_s \rightarrow \infty$  curve, which is the only curve (12) with an horizontal asymptote ( $Kd = \chi^{(m)} \cdot \sqrt{2a/(a-1)}$ ).

A straightforward discussion then shows that all the intercept points of a Brillouin curve shall fall in the positive  $\epsilon_i$  region as far as  $K_b d$  is larger than this asymptotic value  $\gamma_i^{(m)} \cdot \sqrt{2a/(q-1)}$ . This is thus the condition for forward waves and can be rewritten in the form:

$$(K_b d)^2 - (K_p d)^2 > \epsilon_i^{(m)} \gamma_i^{(m)} d^2$$

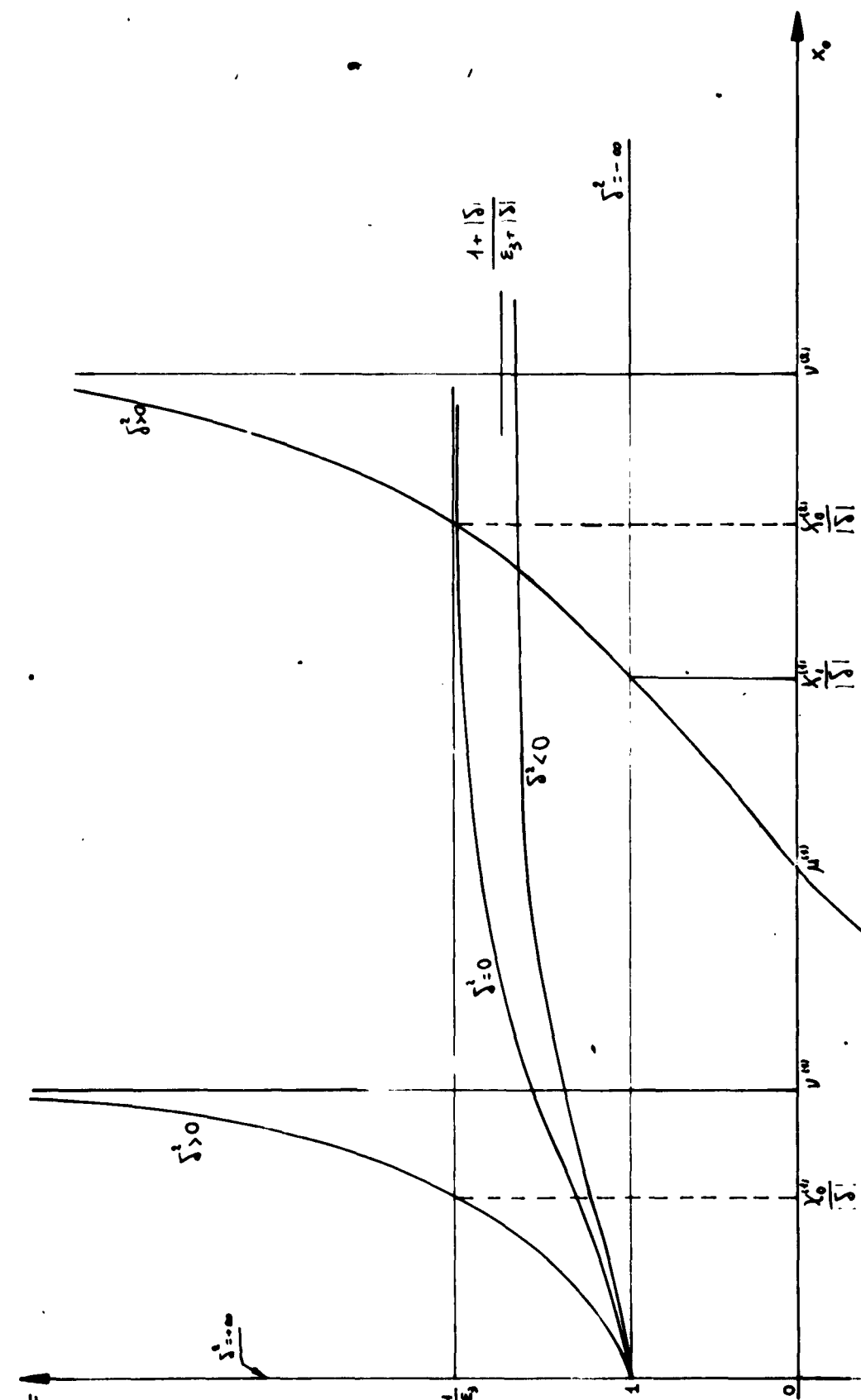
When this condition is not satisfied, the waves may be backward or start at low  $\beta d$  values as forward and change to backward at large  $\beta d$  values.

BIBLIOGRAPHY

---

- 1) - A.I. Akhiezer et al. - Proc.U.N. Conference on the  
Peaceful Uses of Atomic Energy  
Vol.31, pp.225 (Geneve, 1958)
- 2) - W.C. Schumann - Z. Angew. Phys. 10 26(1953)
- 3) - A.W. Trivelpiece and R.W. Gould - J. Appl. Phys. 30  
1784 (1959)
- 4) - L.U. Smilin and P. Chorney - Proc. Poly. Inst. of  
Brooklyn Symposium, April 1958

Fig. 1



foglio di

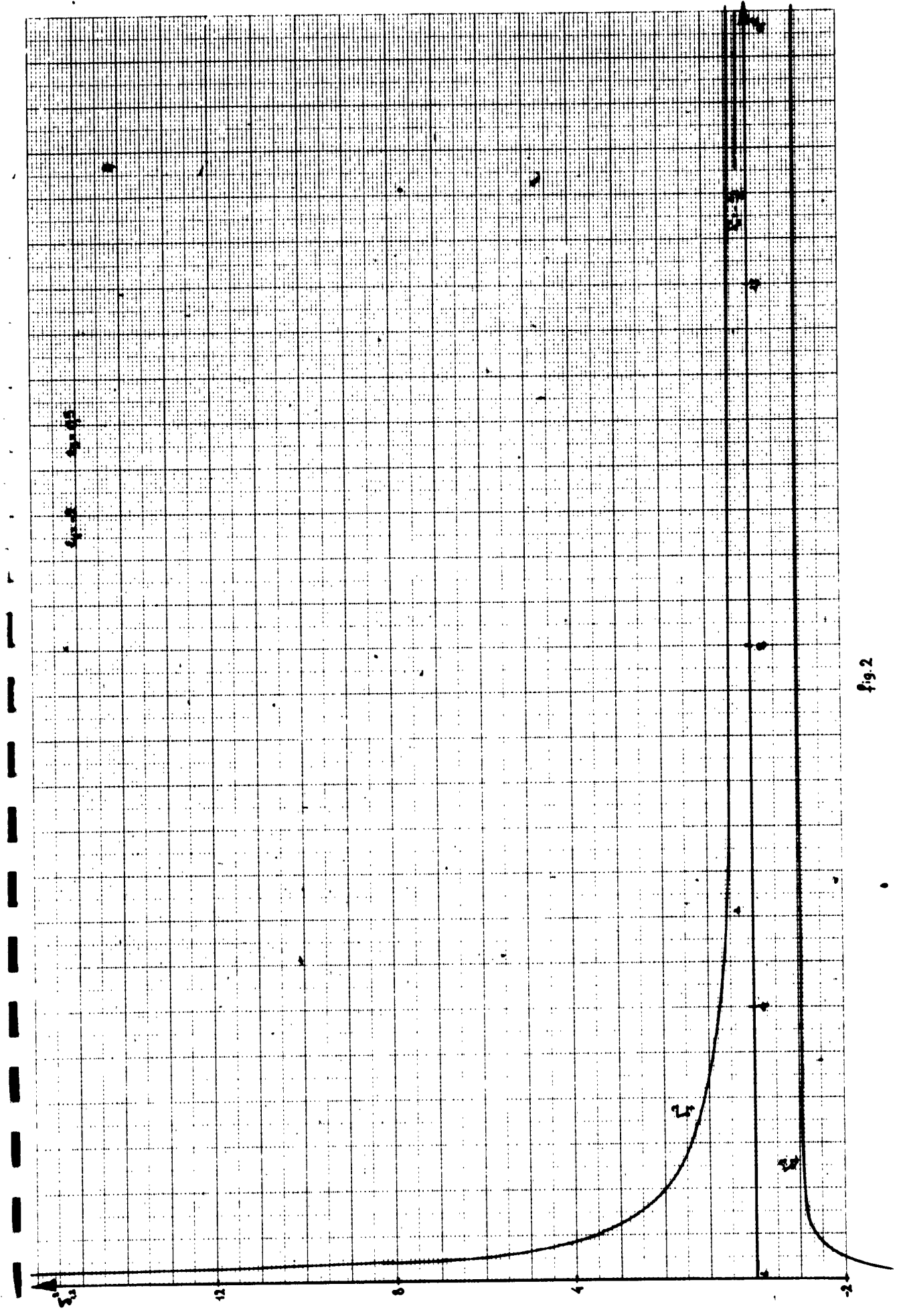


Fig. 2

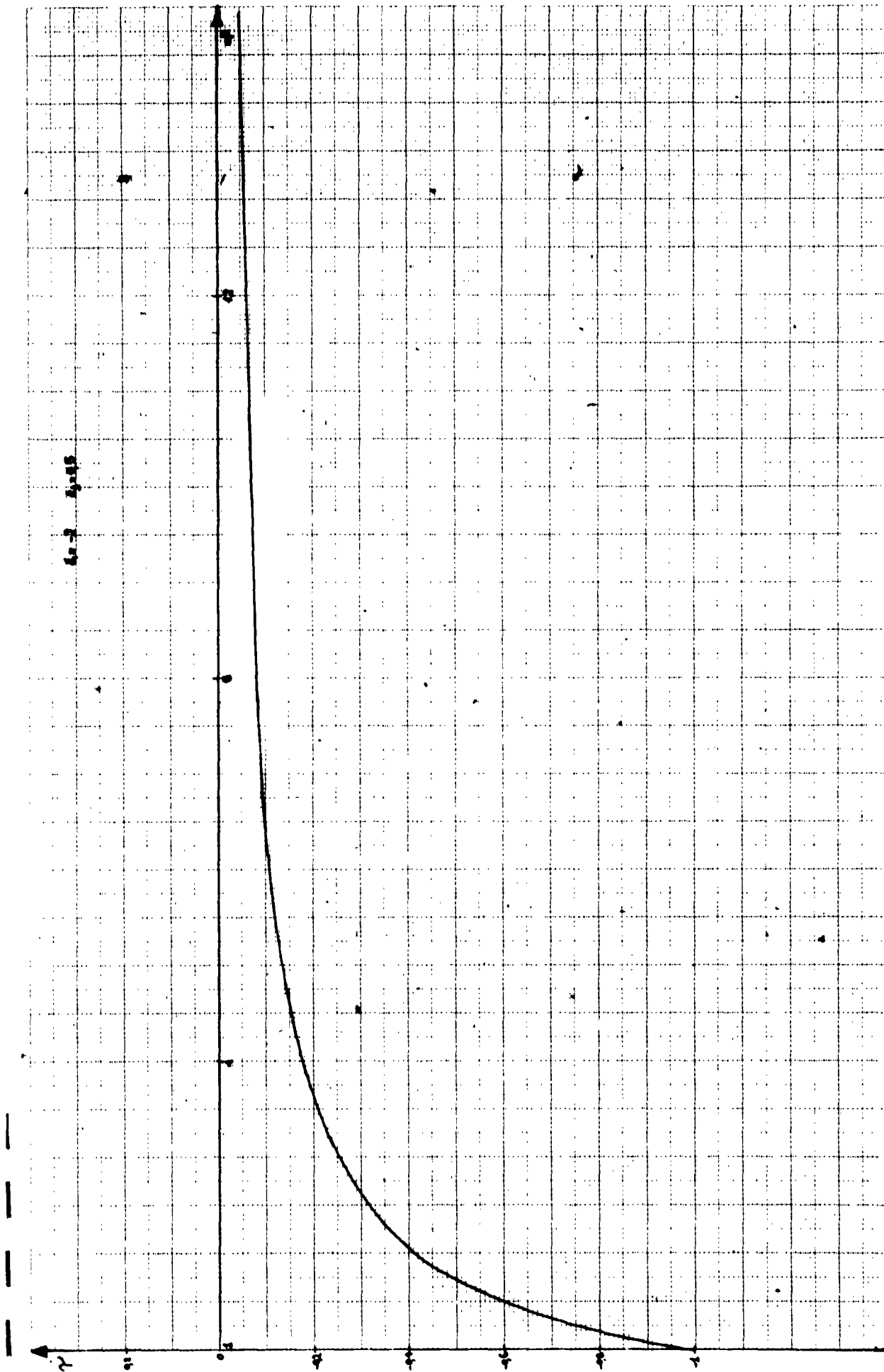


Fig. 3

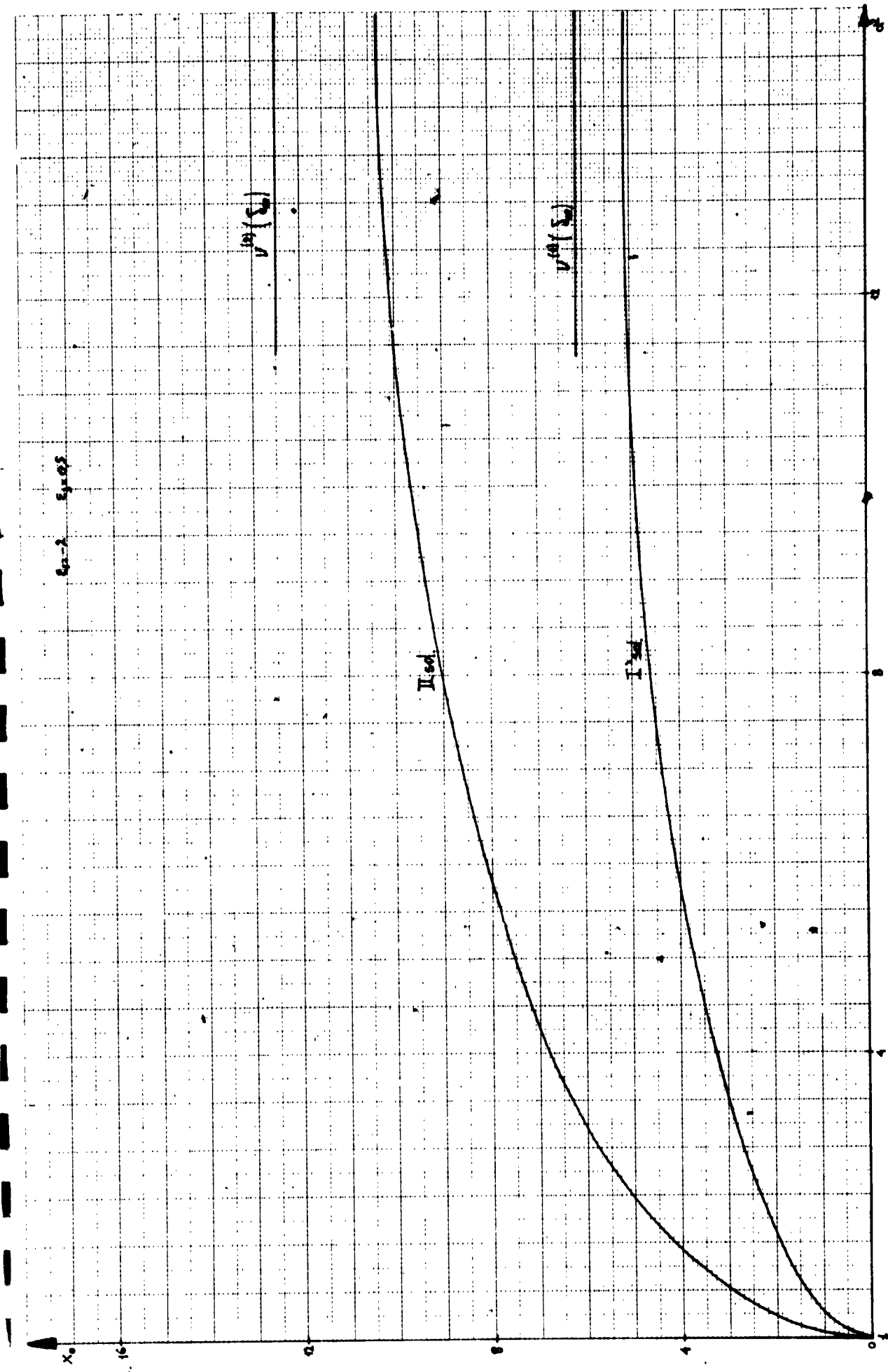
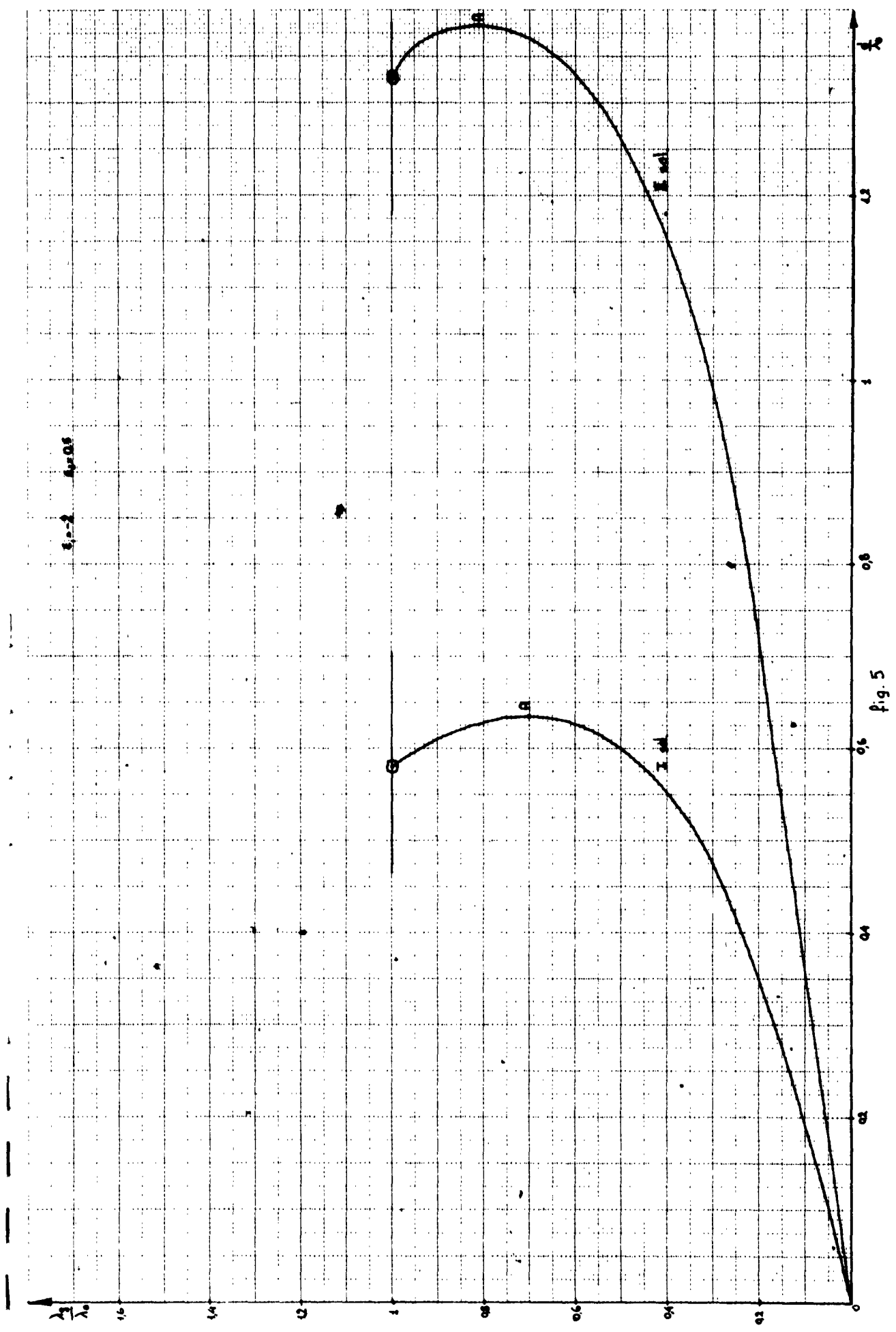
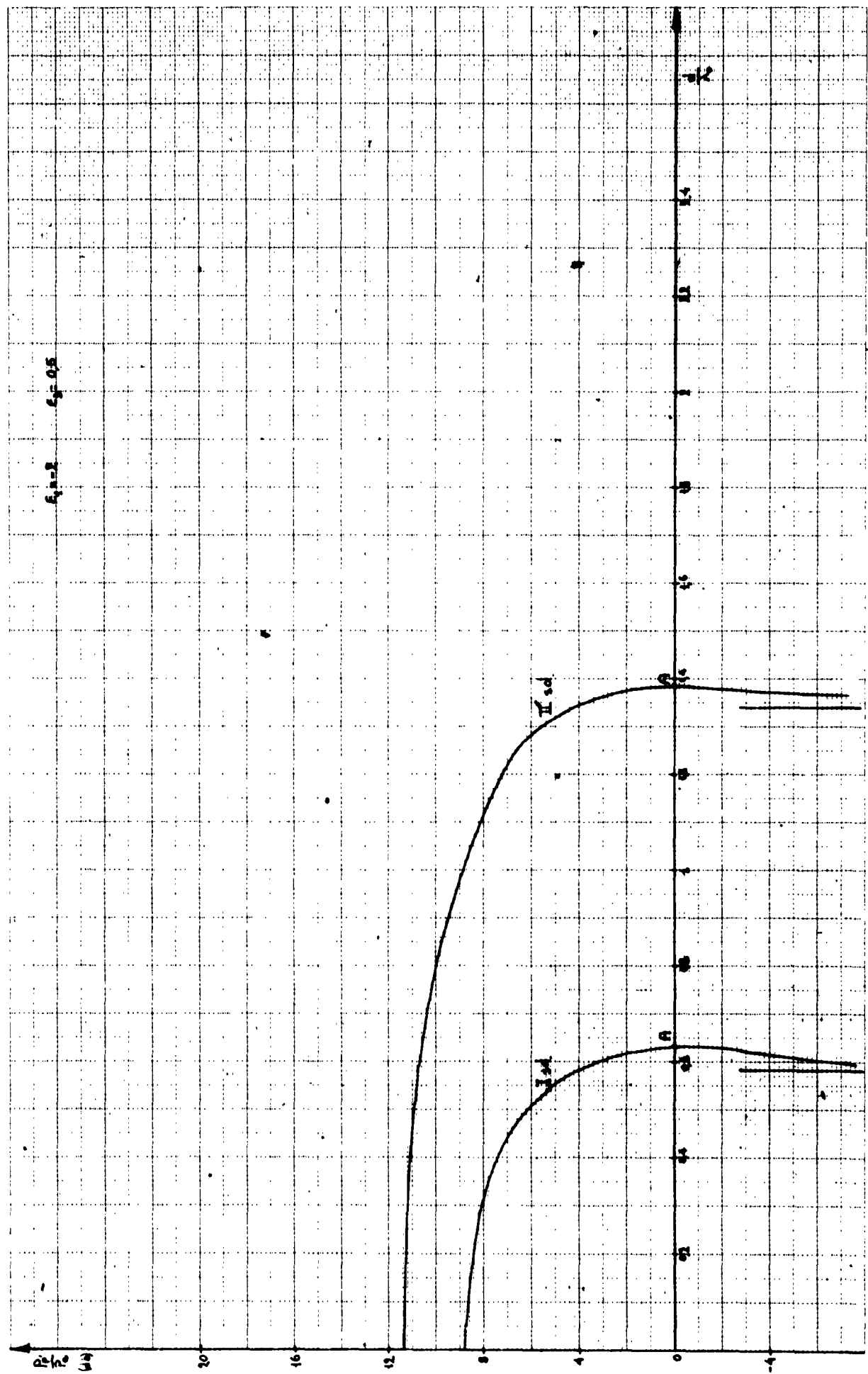


fig. 4





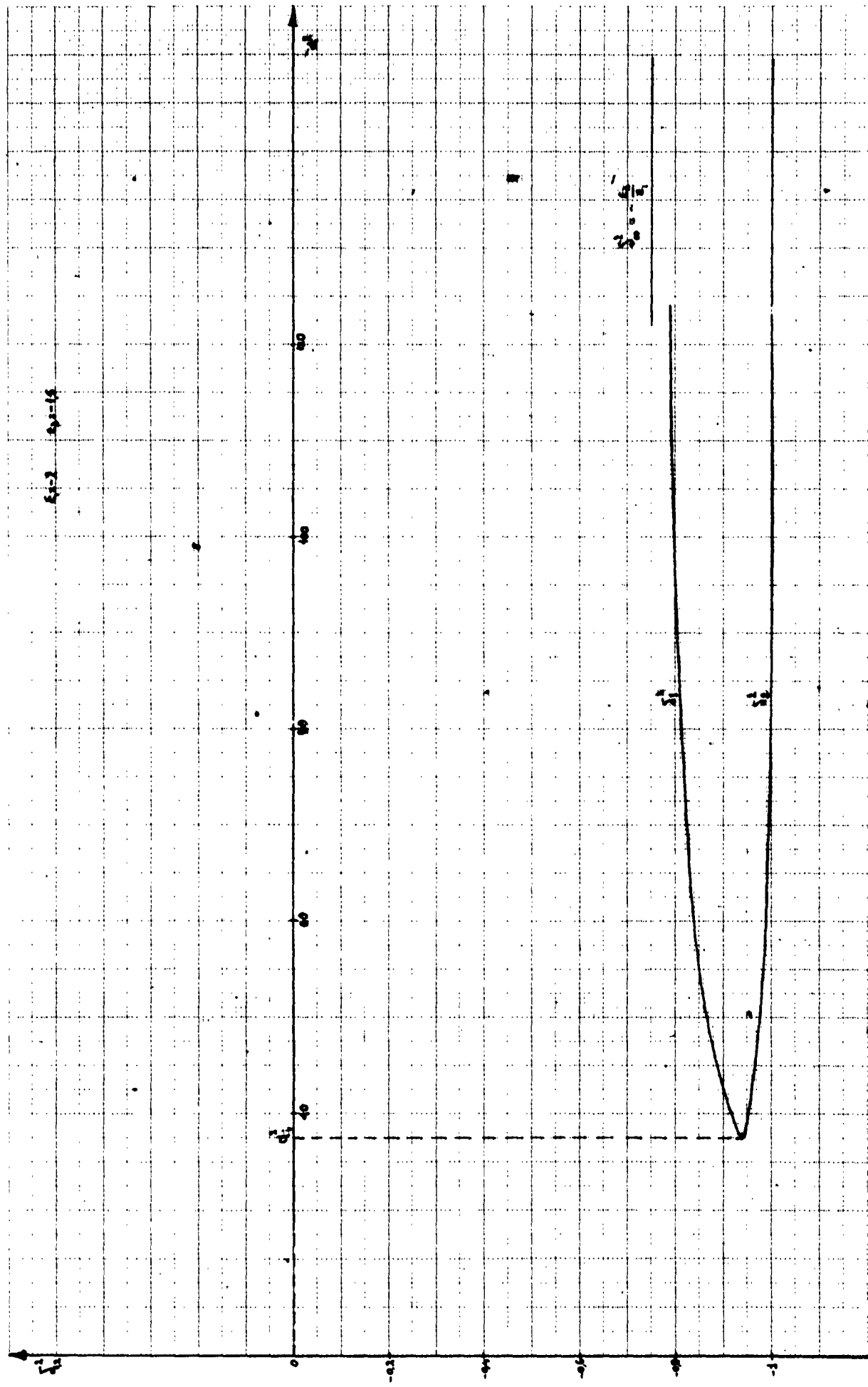
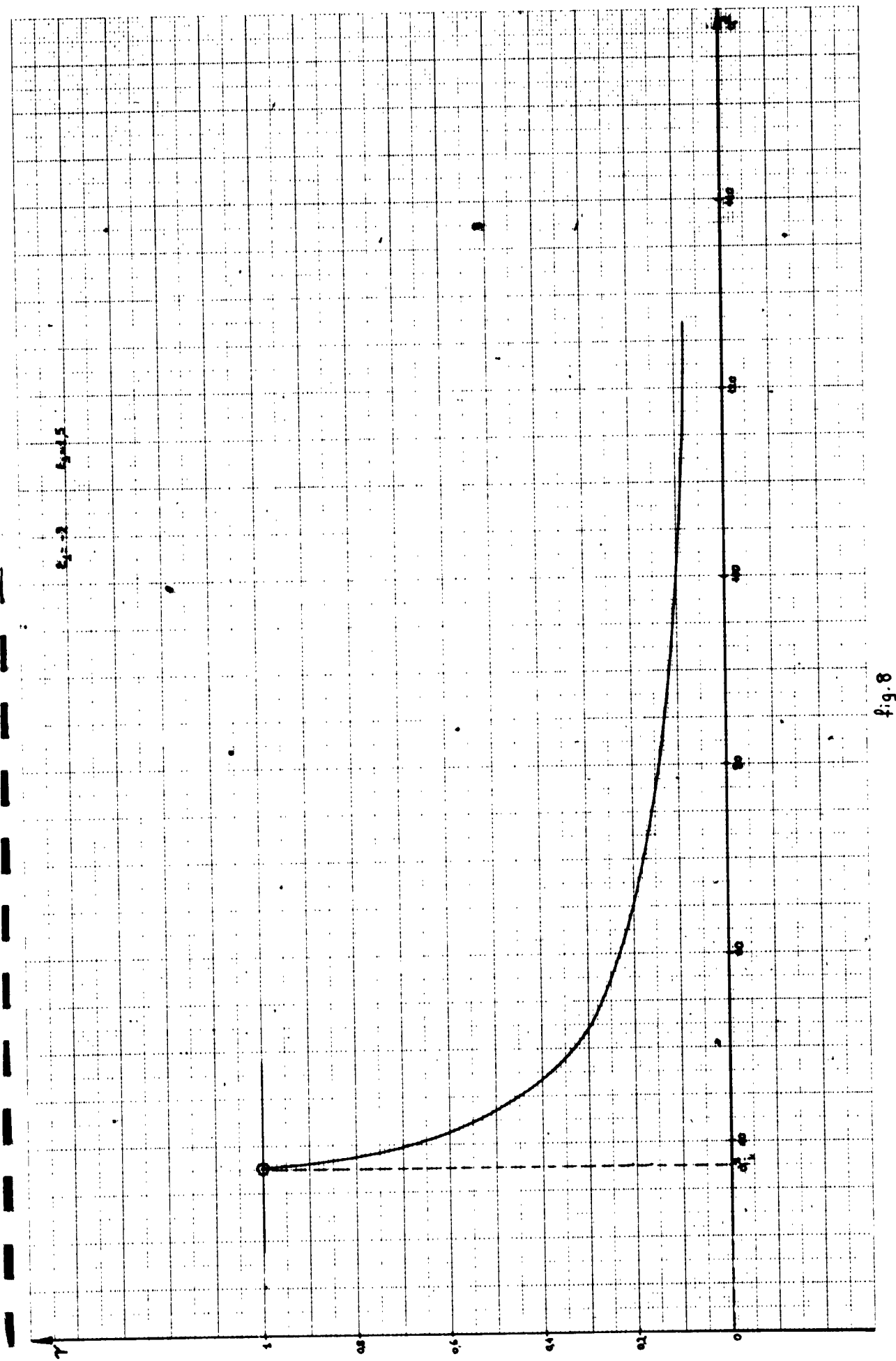


fig. 7



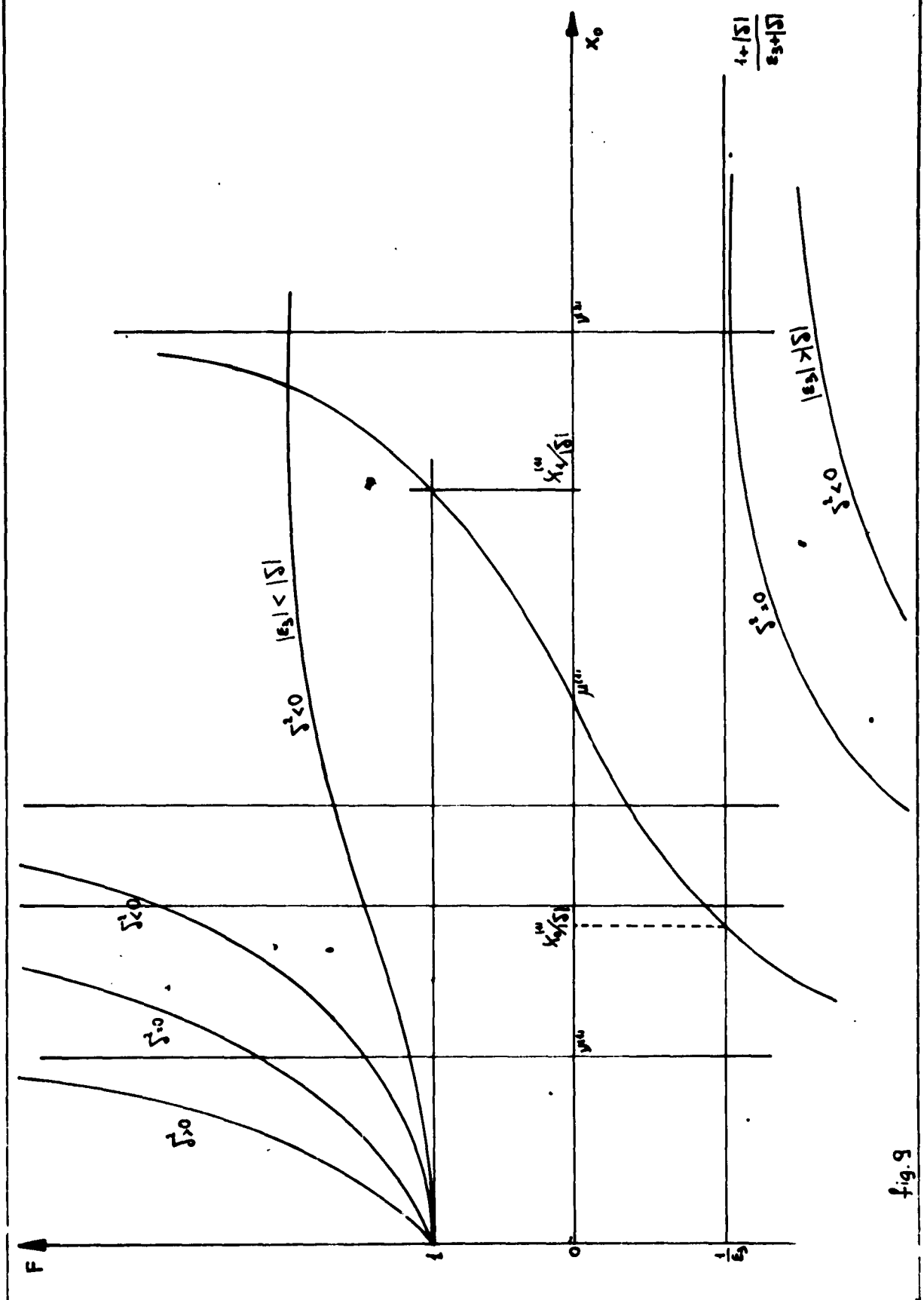


fig. 9

foglio di

Fig. 10

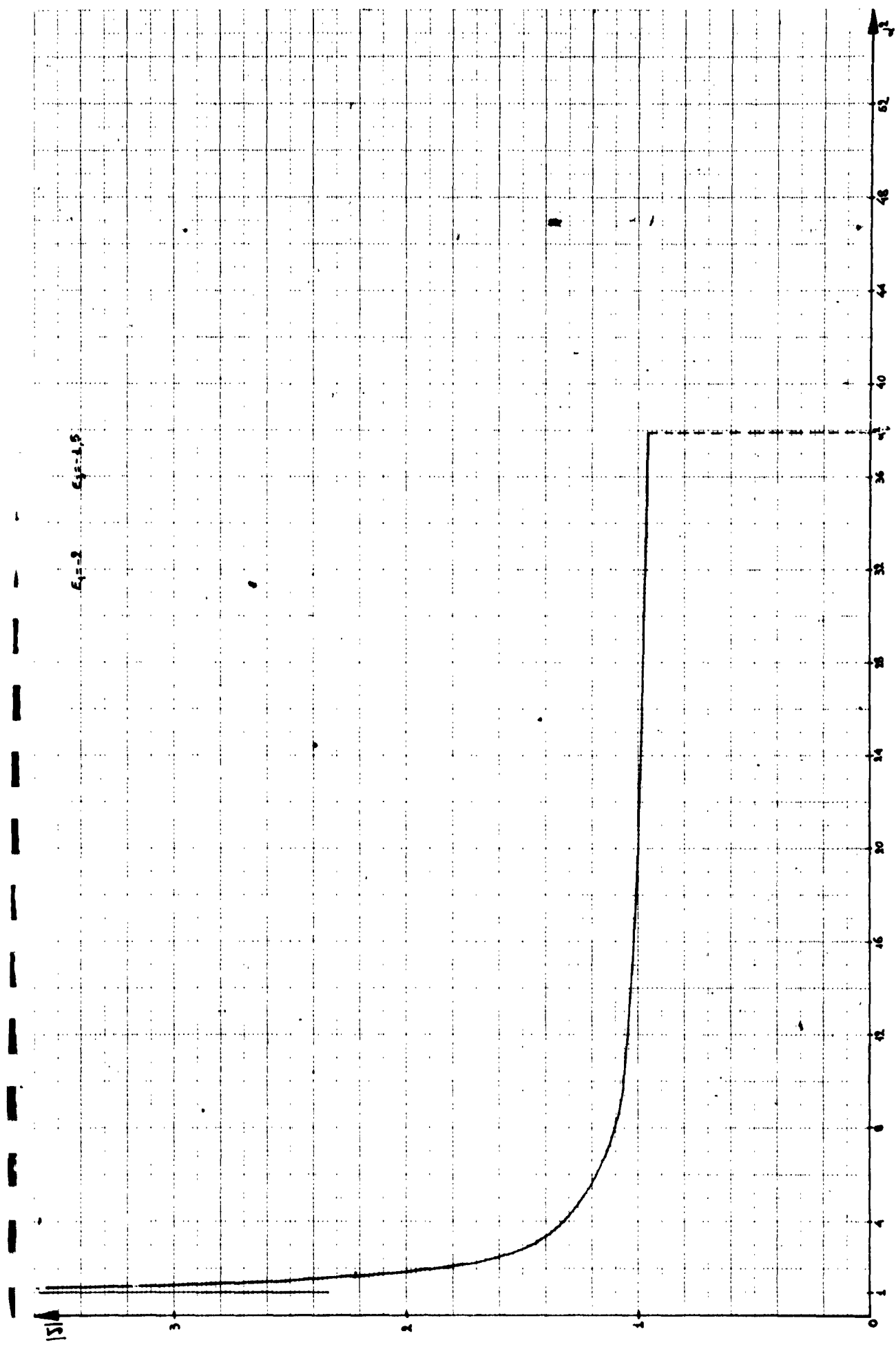
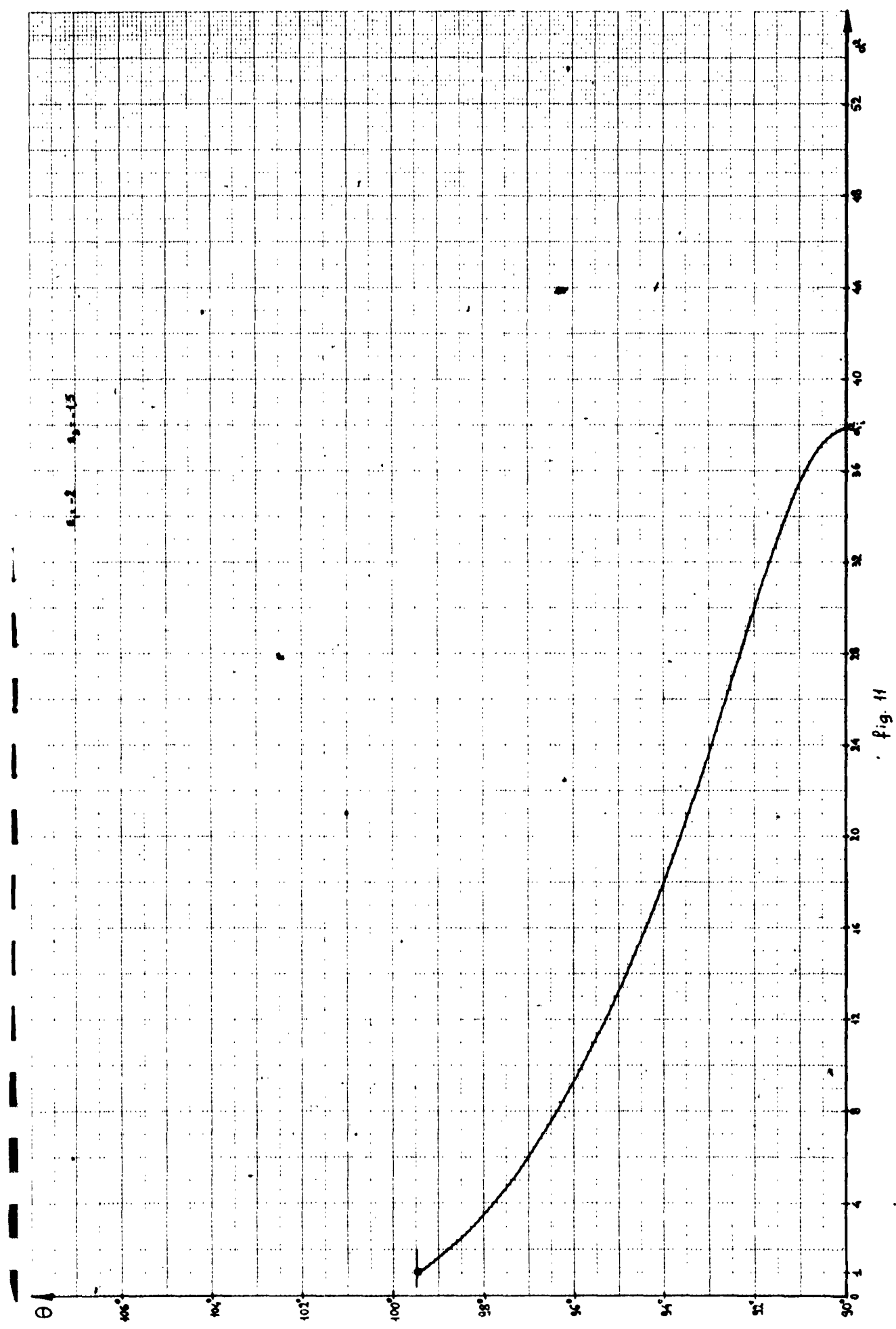
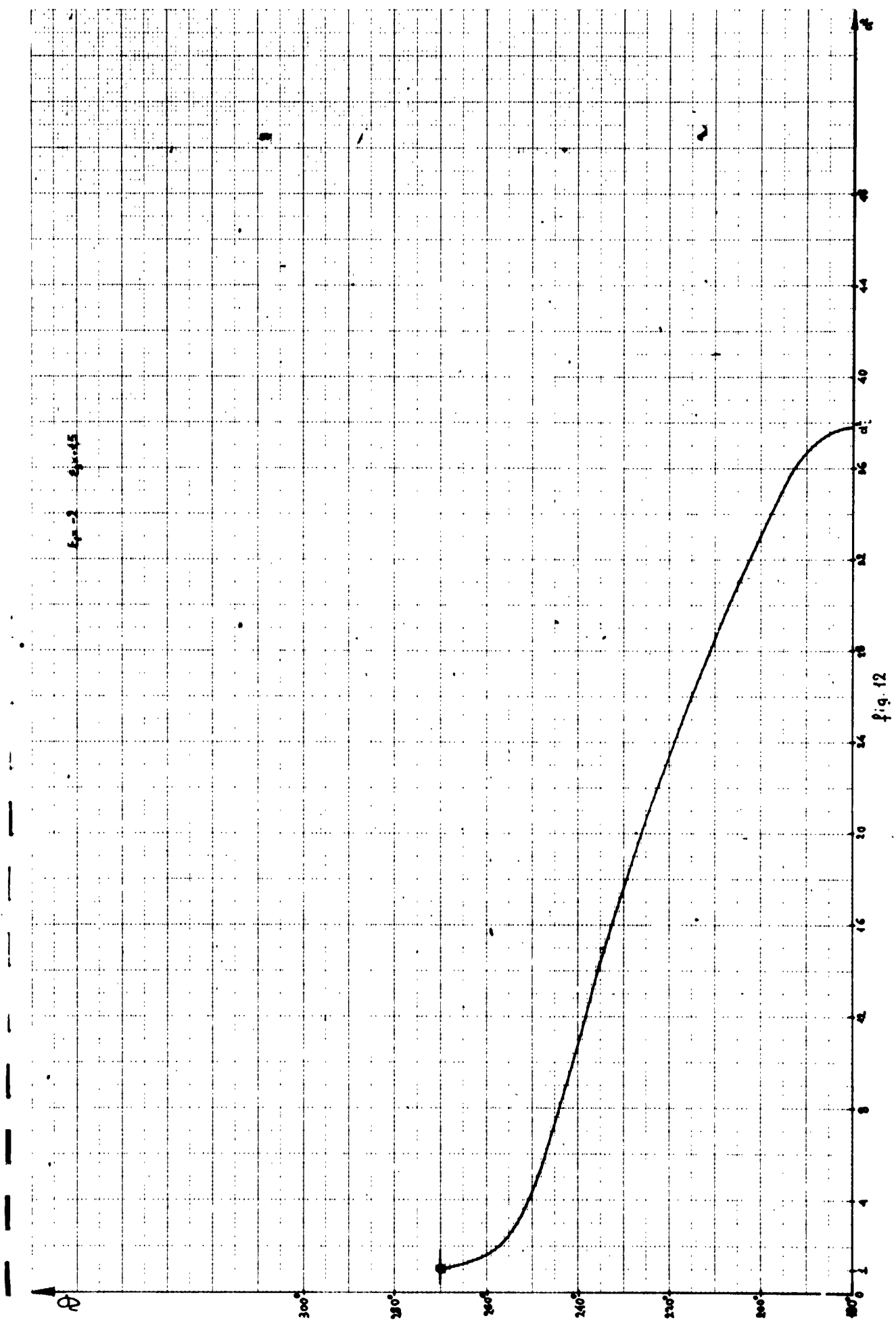
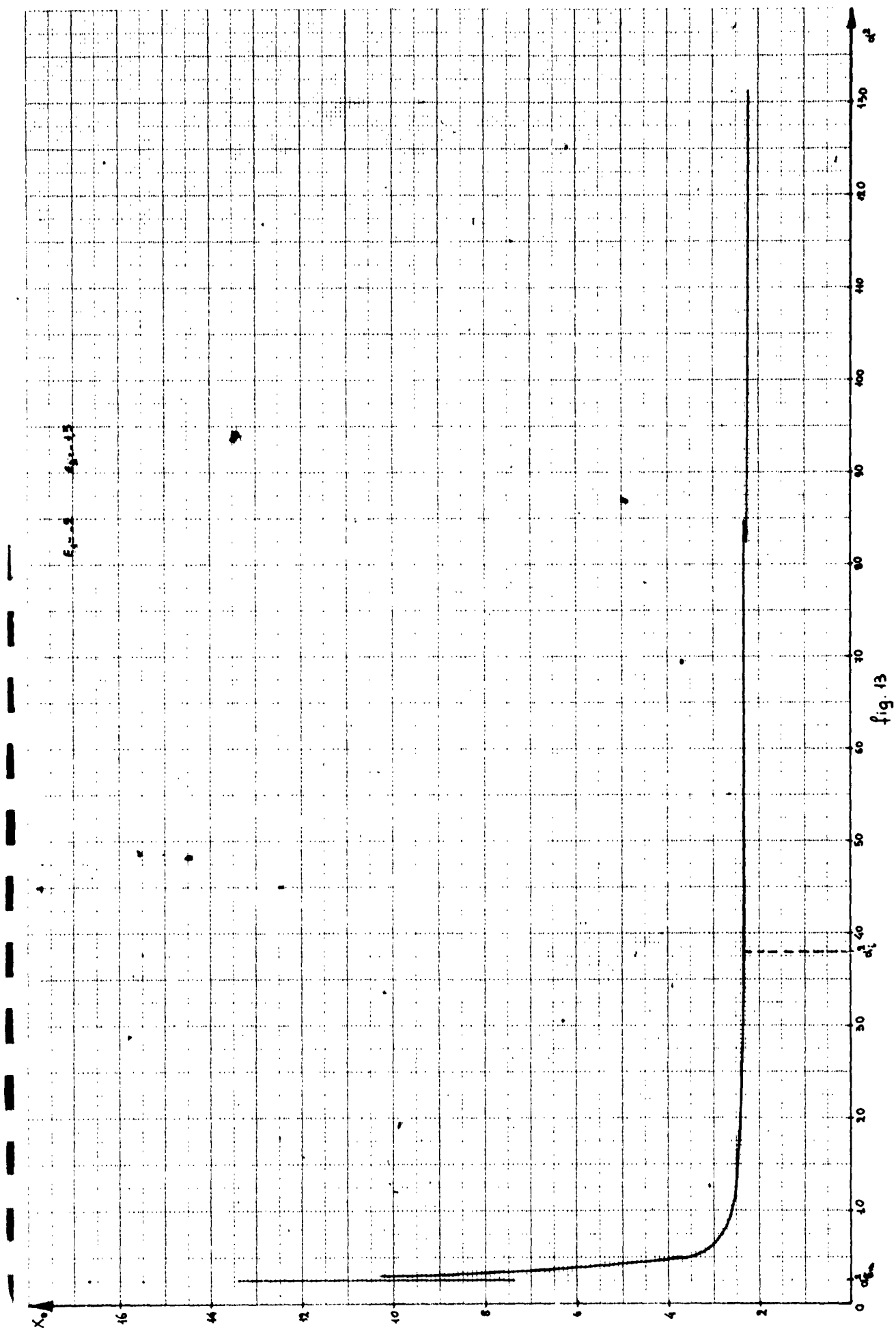
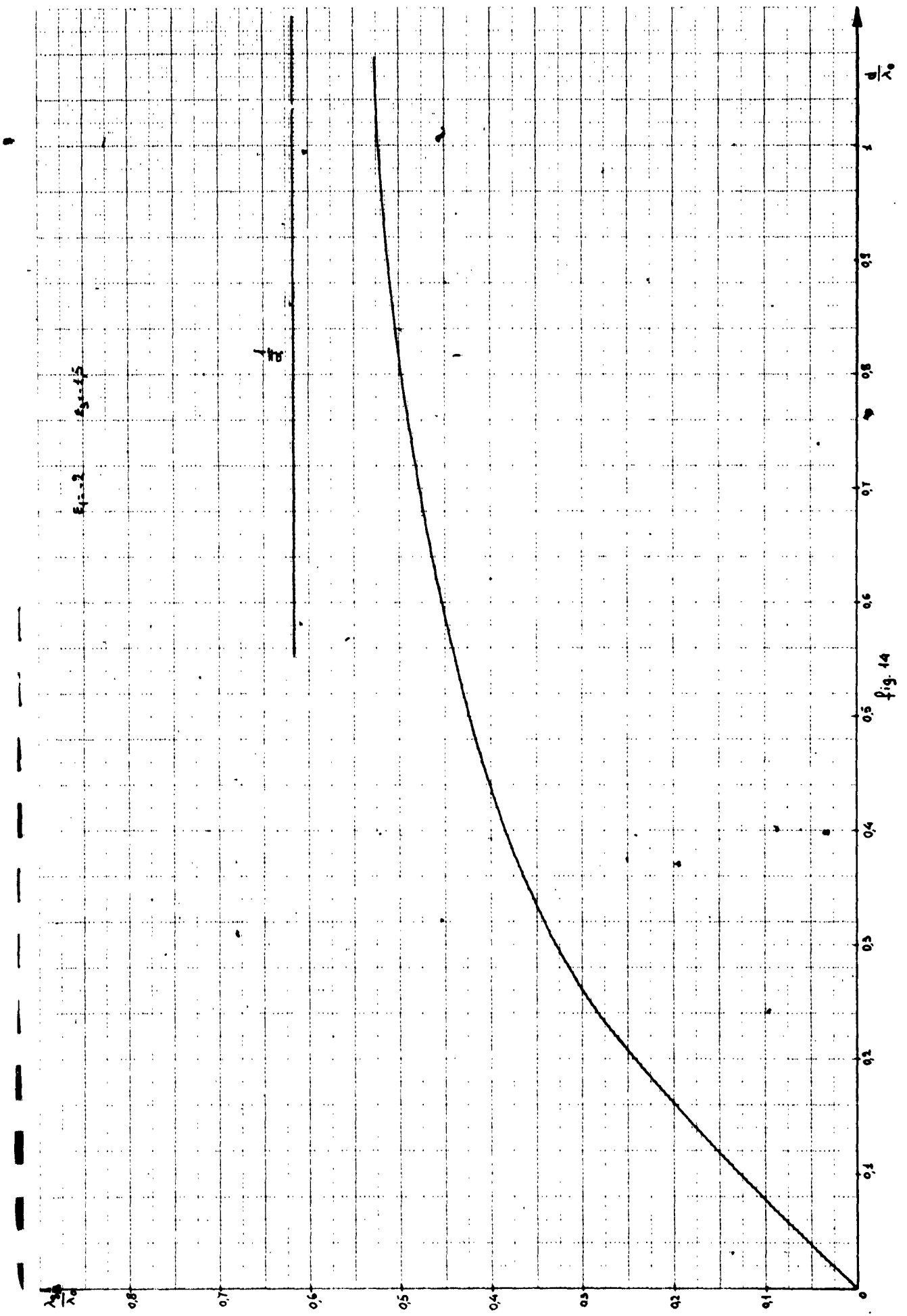


Fig. 9









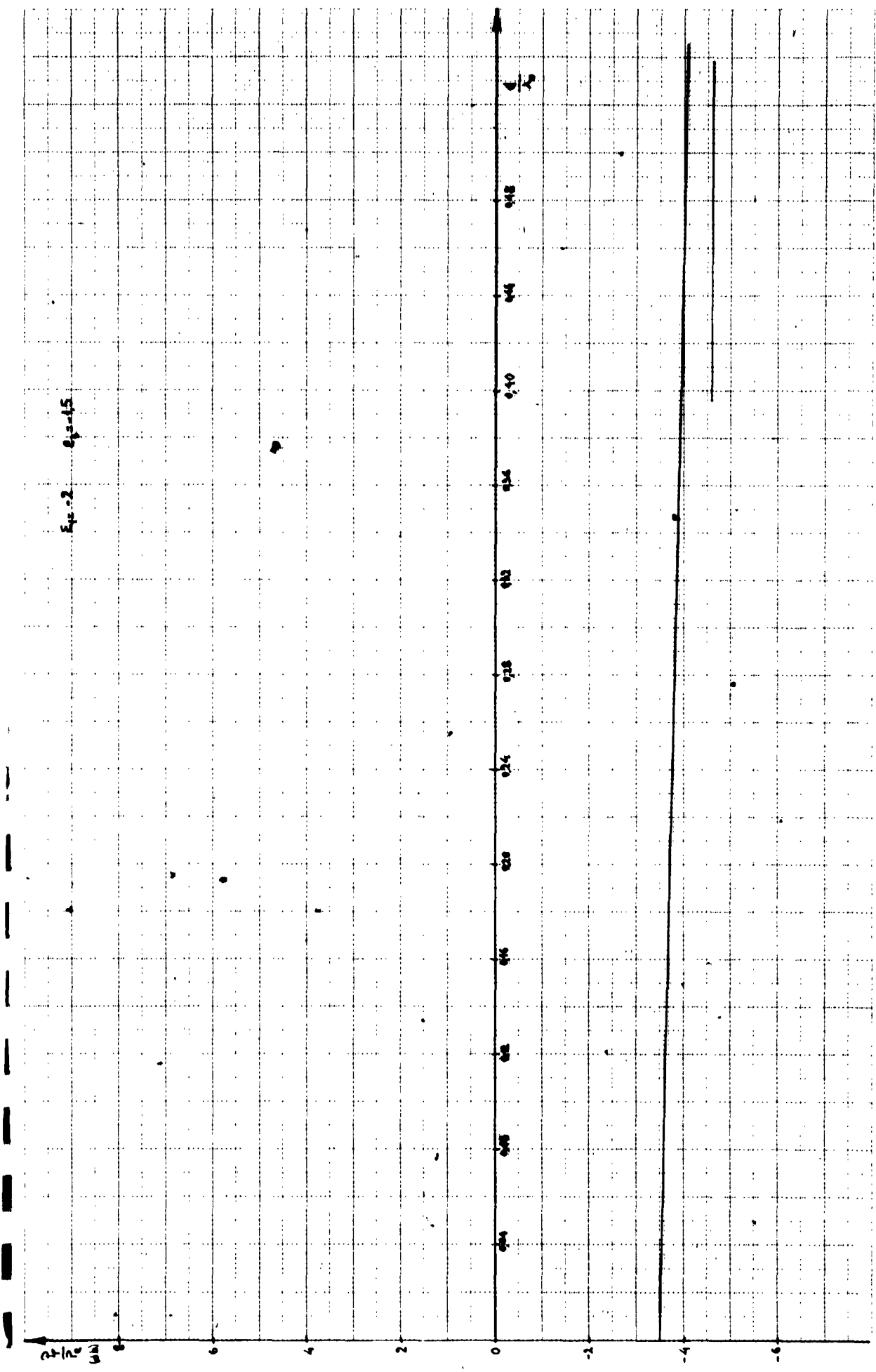


Fig. 15

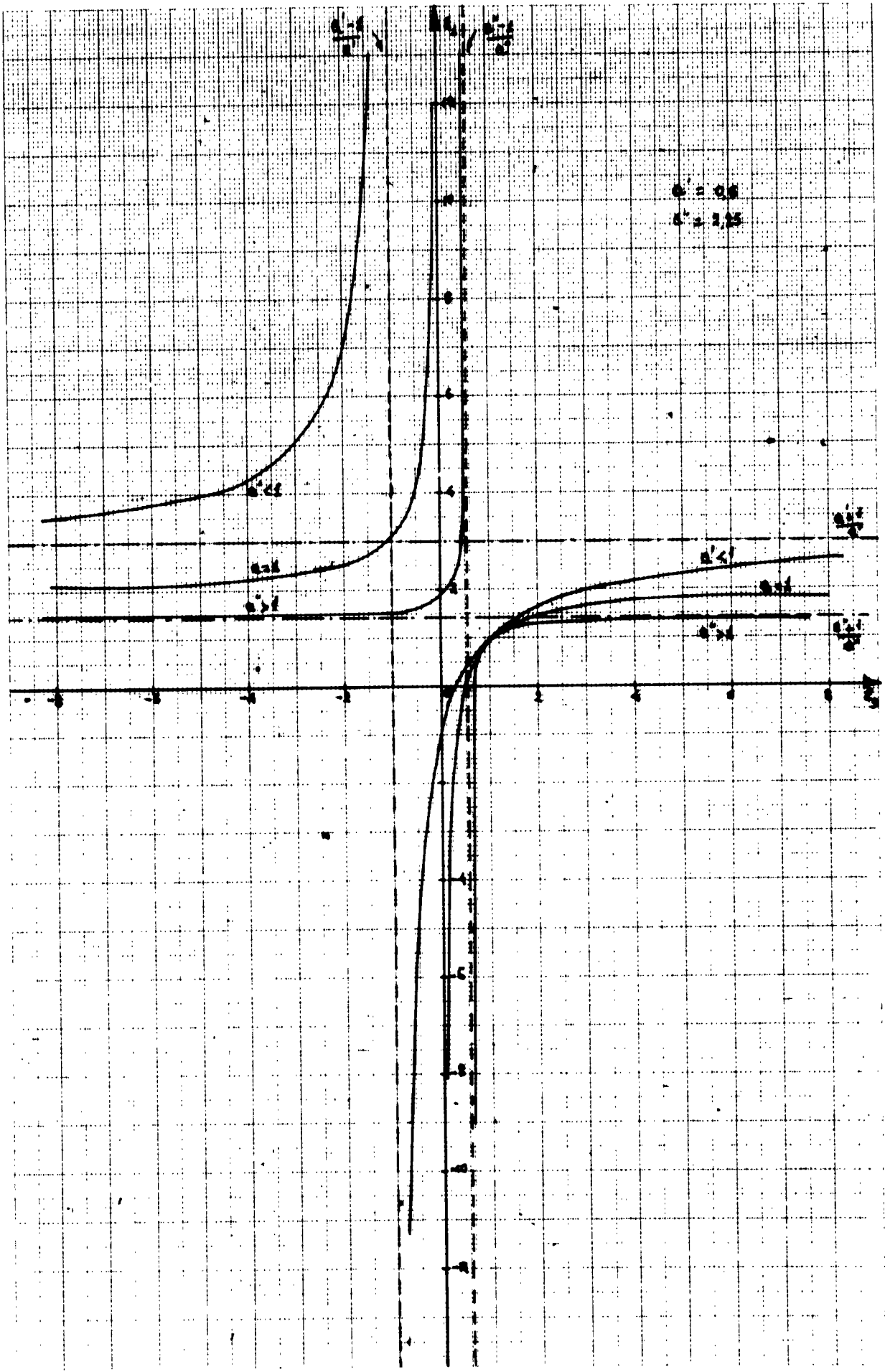
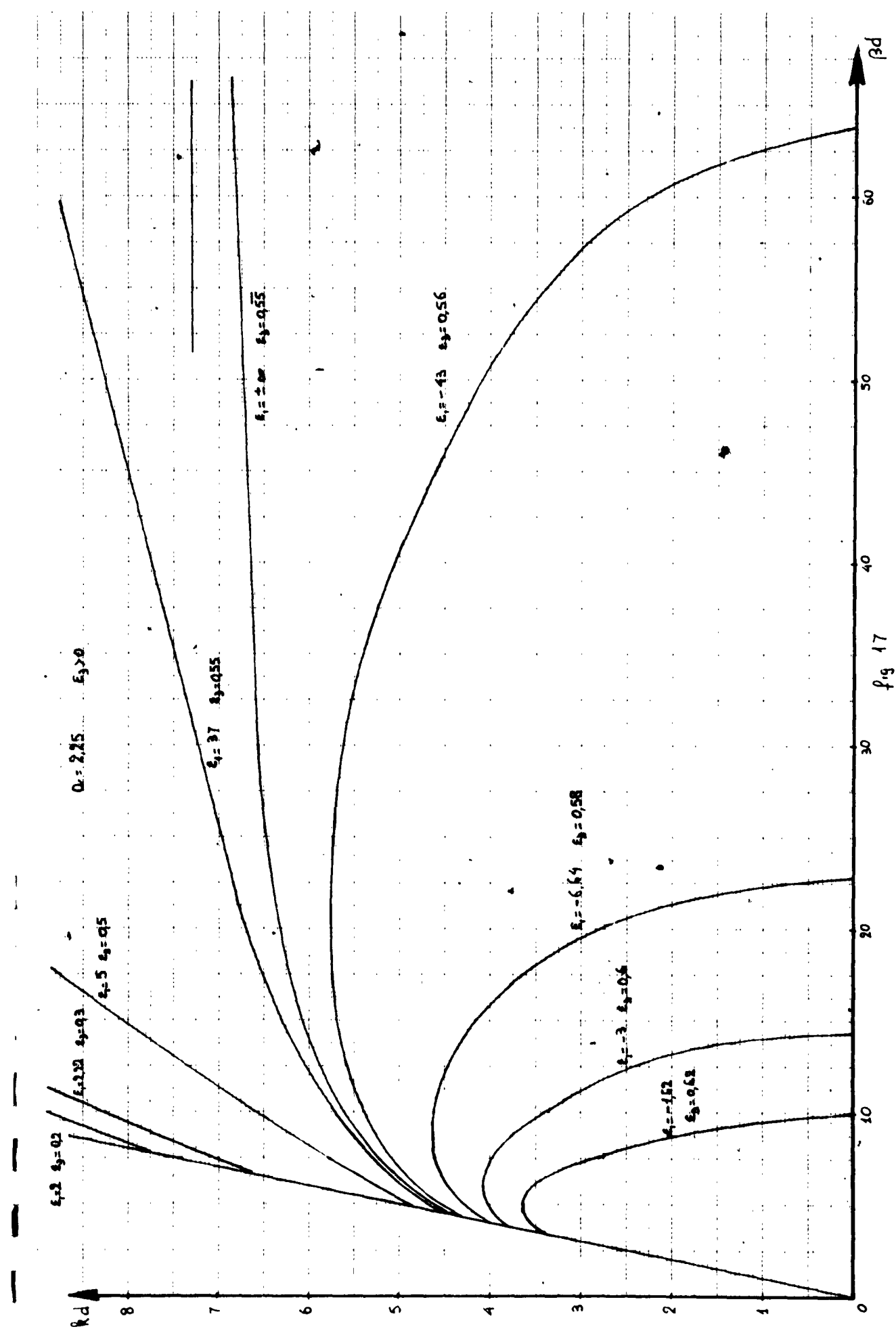
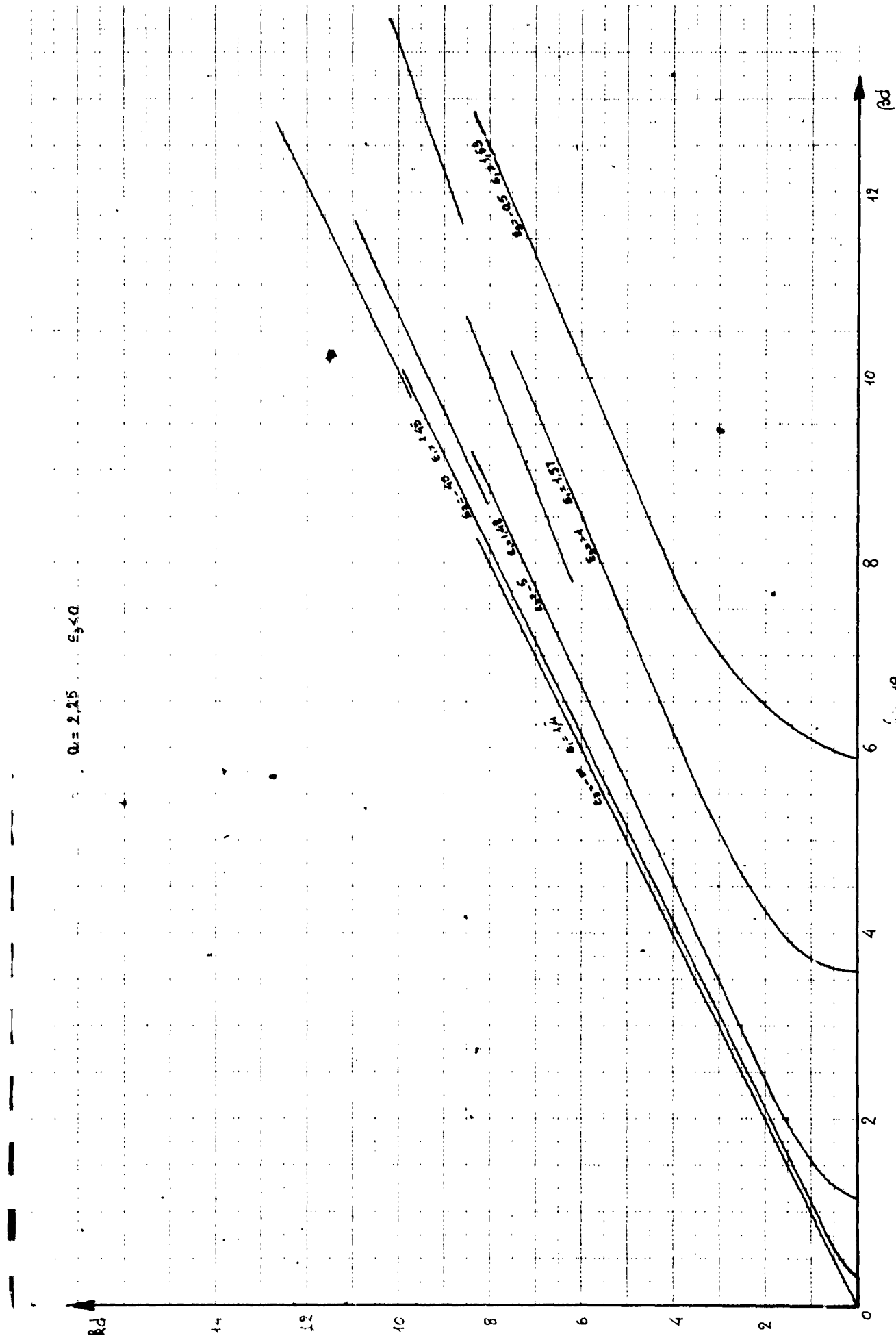
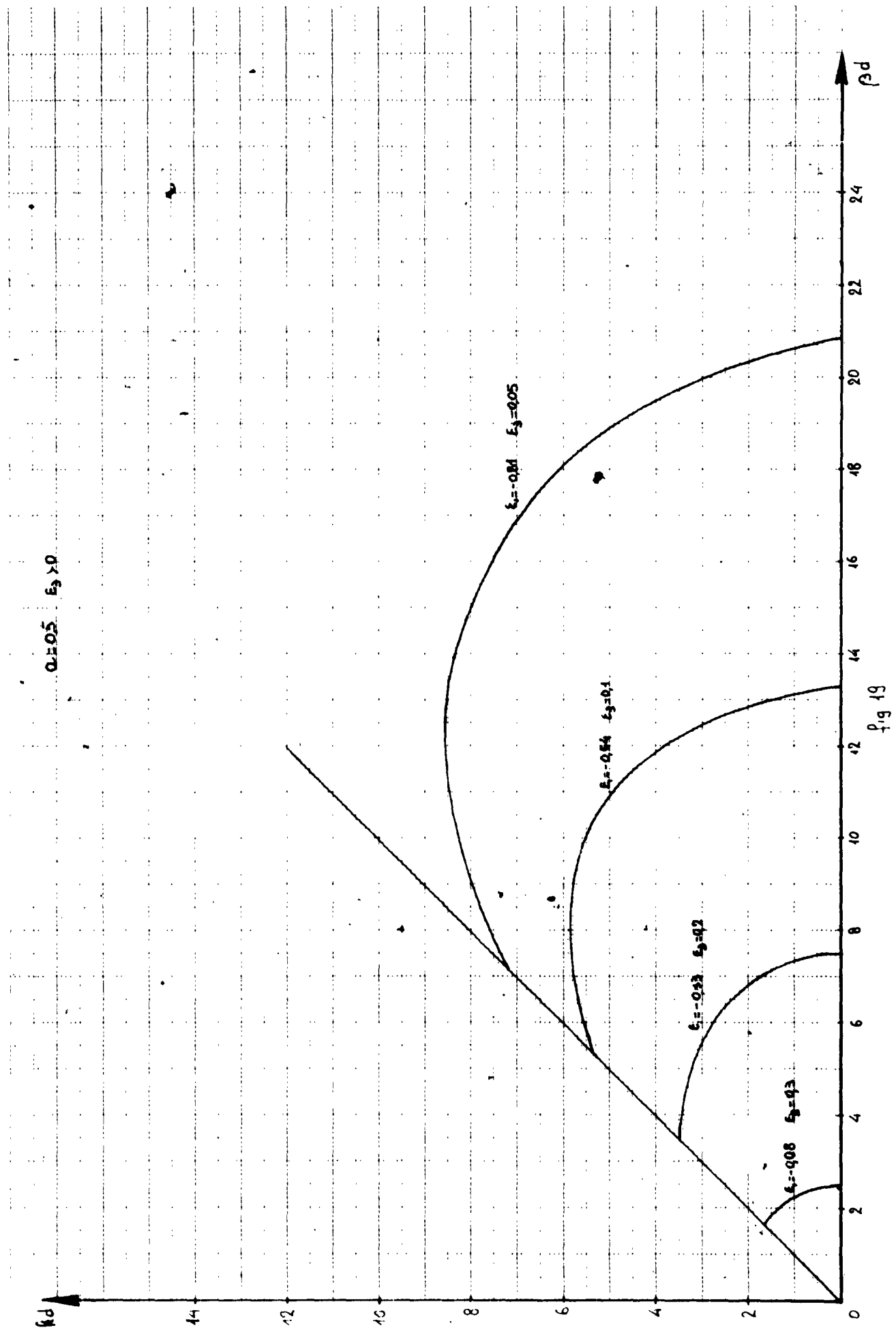
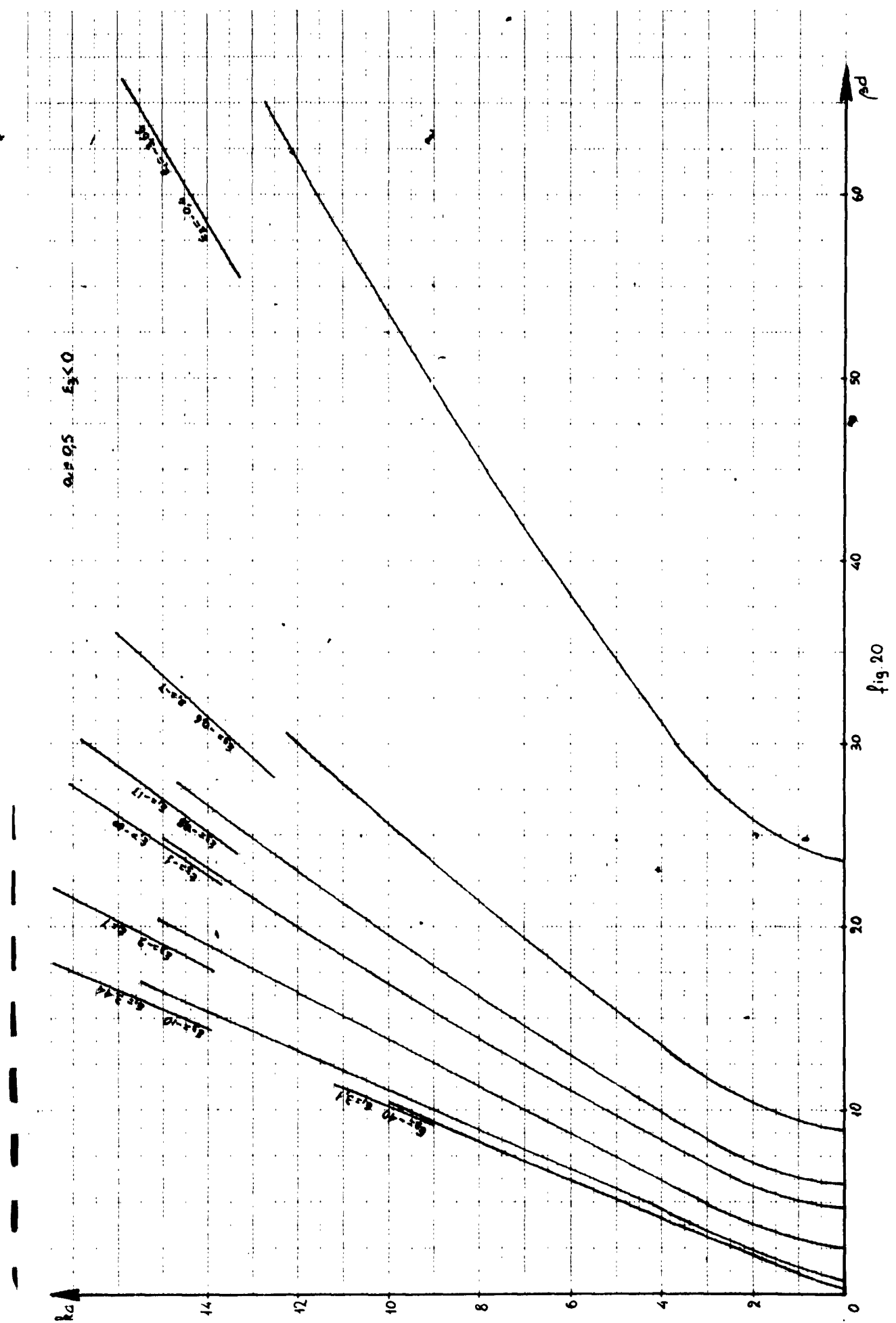


fig.16









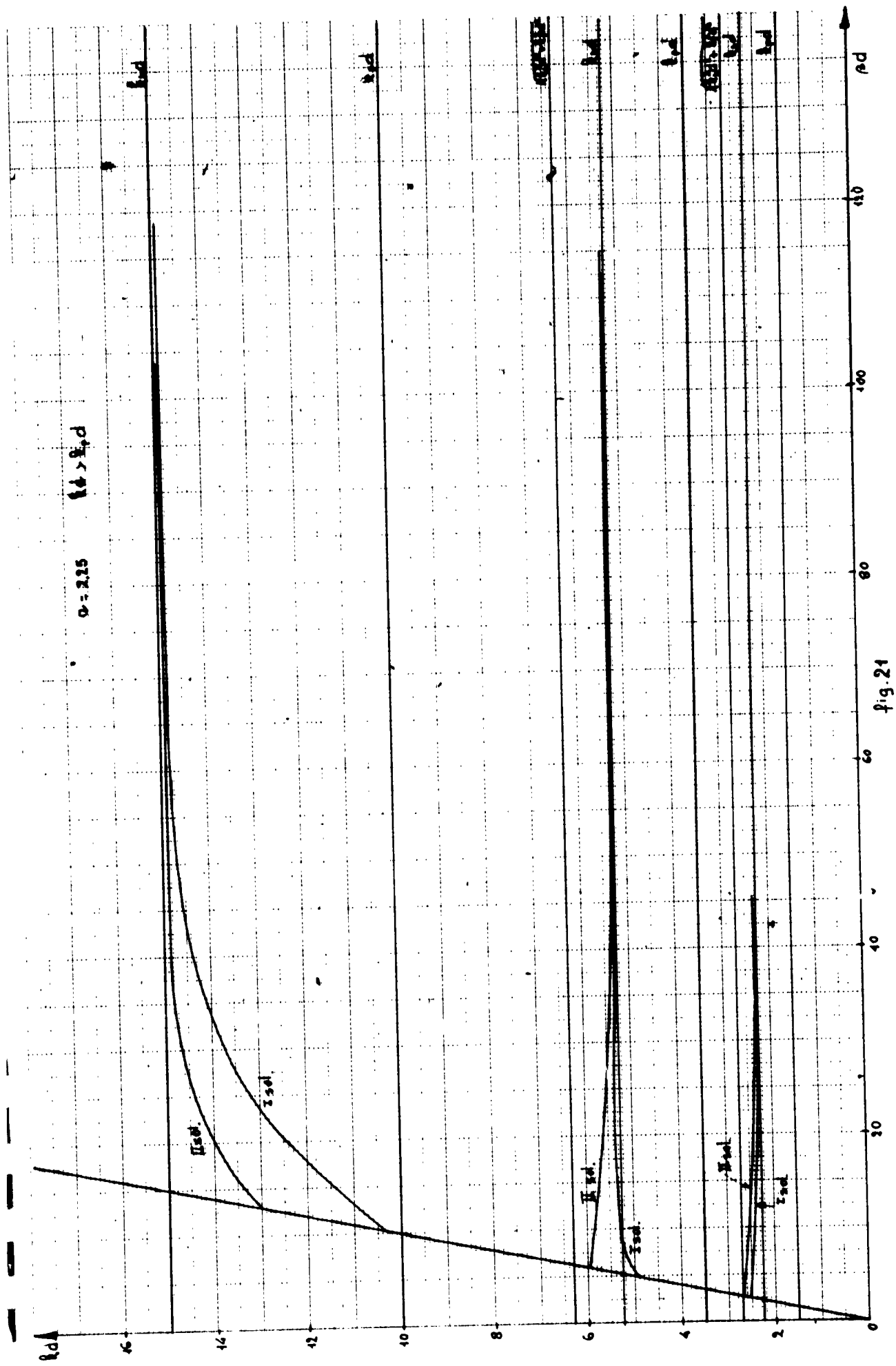
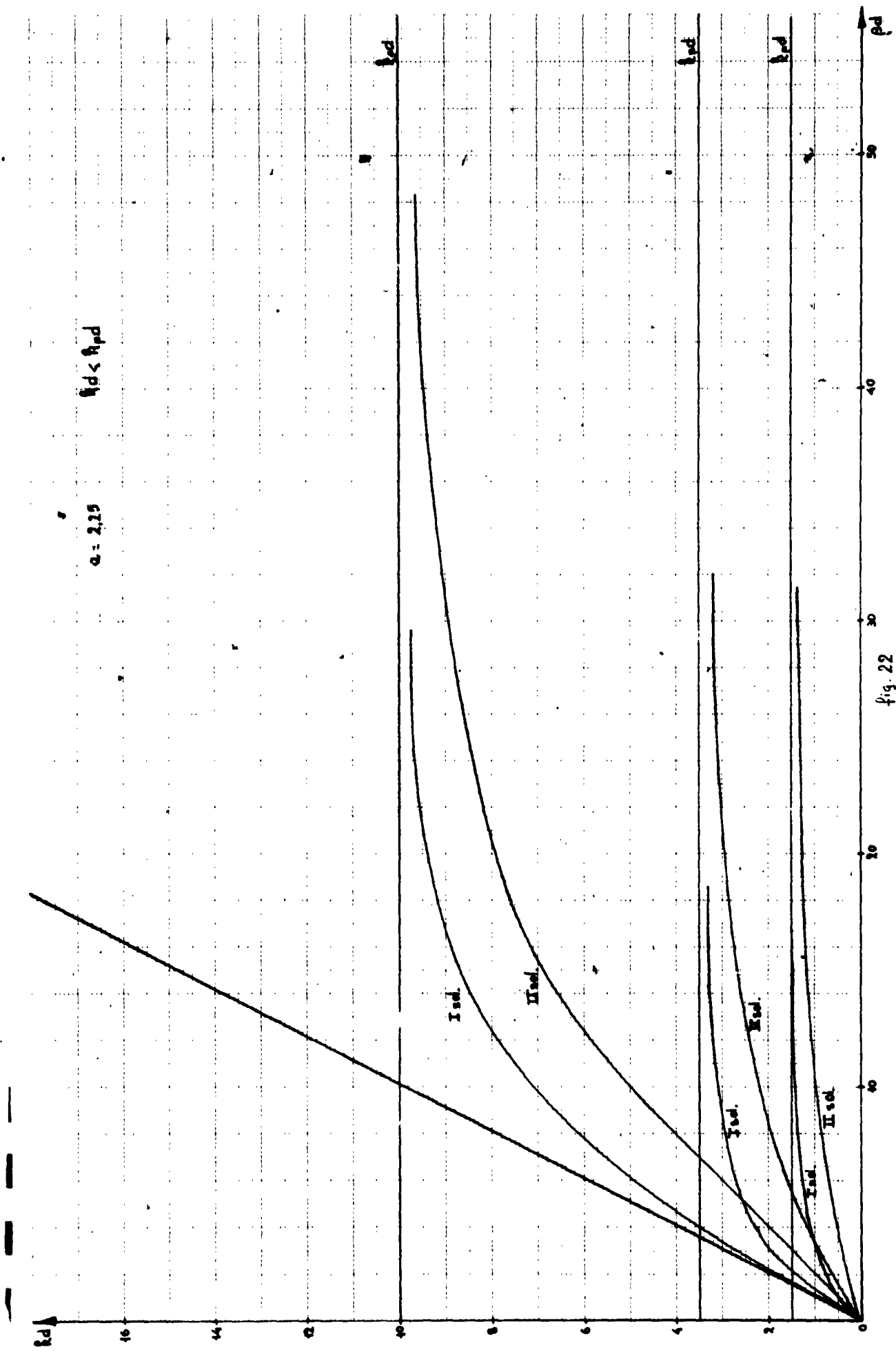
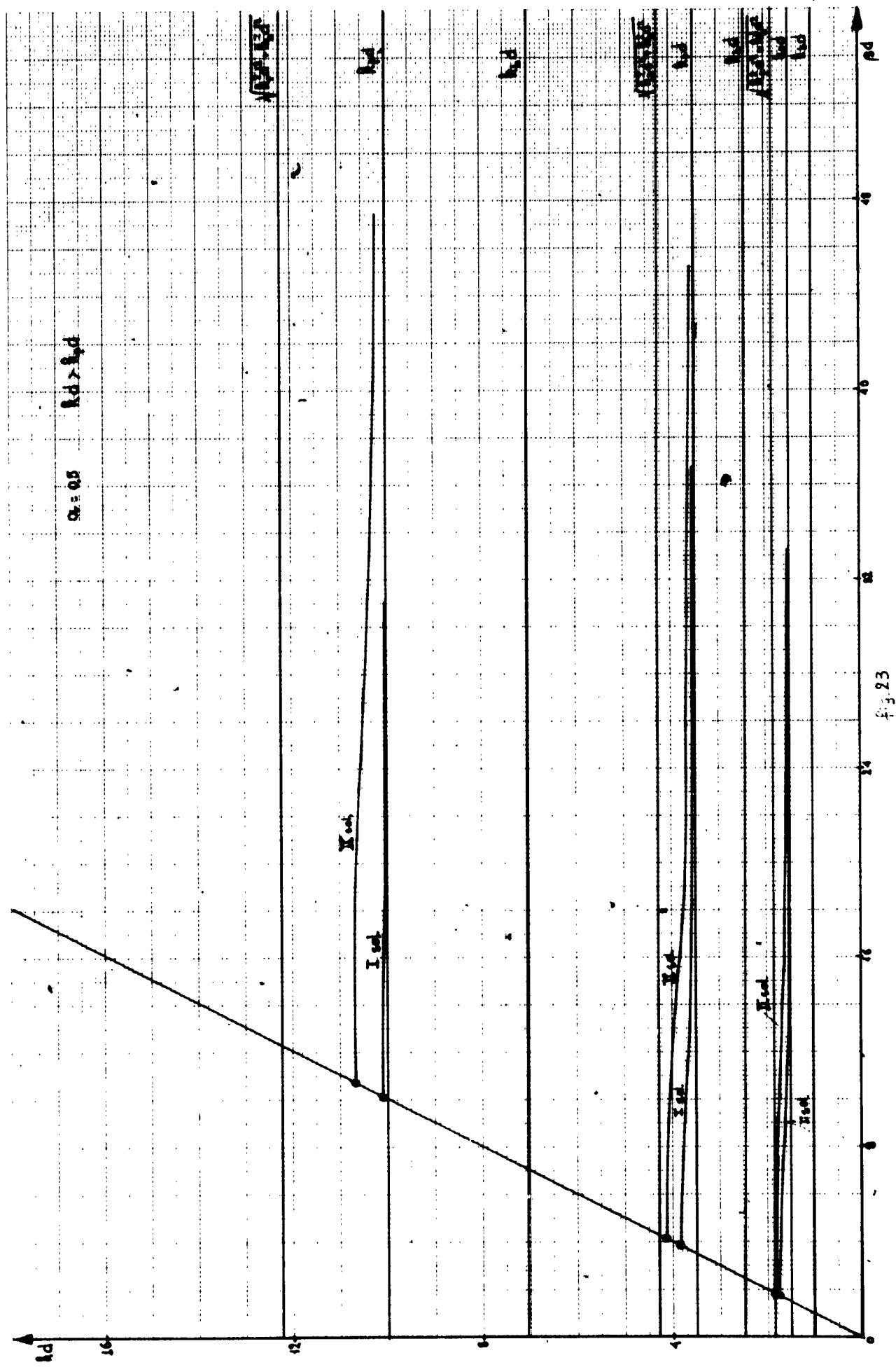
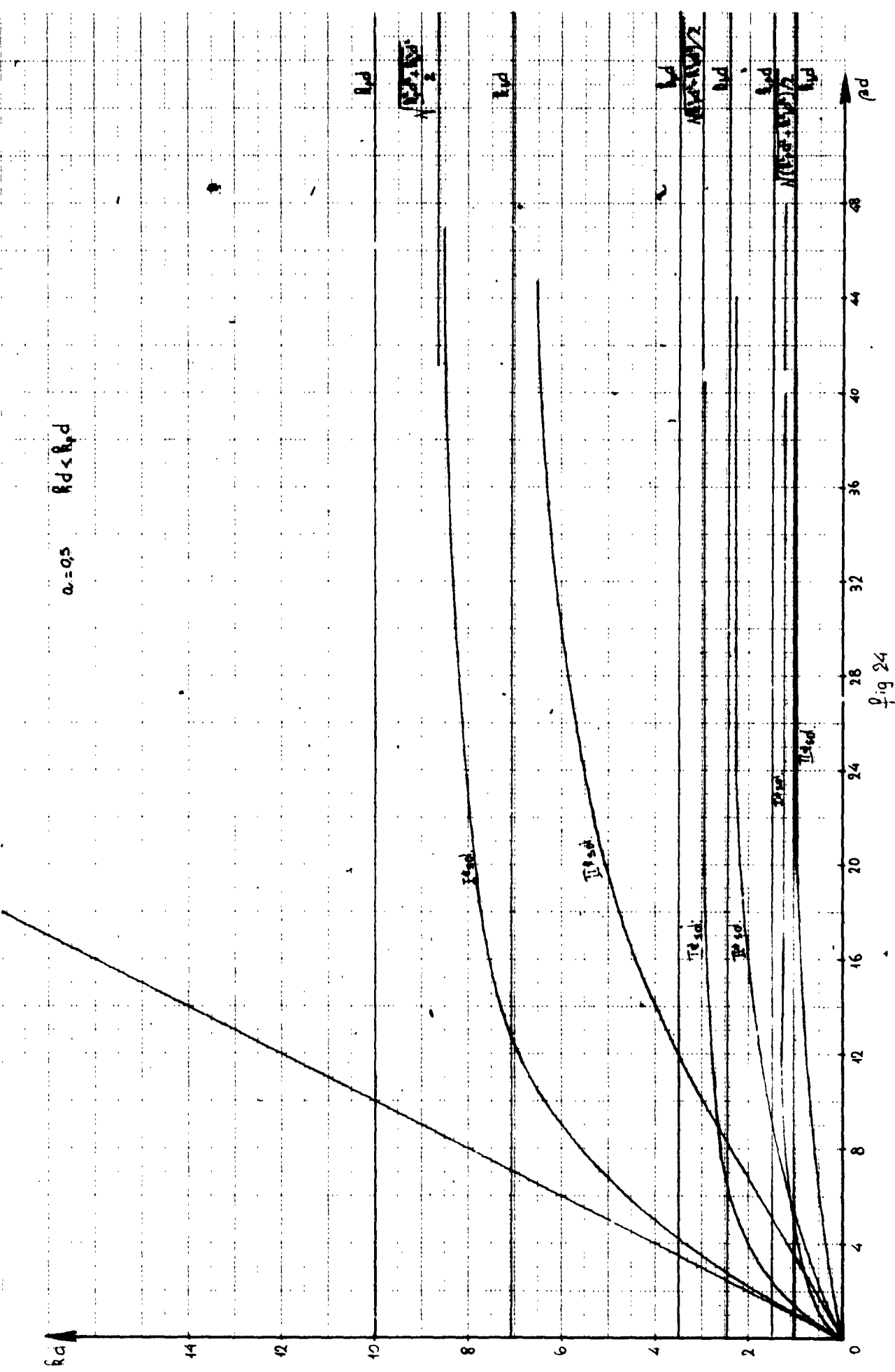


fig. 22







ASTIA NO.  
Contract No: AF 61 (052) - 145  
United States Air Force, Air Research and  
Development Command, European Office,  
Brussels, Belgium

Technical (Scientific) Note No. 2

TITLE: "PROPAGATION CHARACTERISTICS OF A MAGNETO-IONIC DUCT"

By: D. Formato and A. Gillardini

Date: 1 May, 1961

Pages: 39

Organization: SELENIA S.p.A., Via Tiburtina Km 12,400, Rome, Italy

ABSTRACT: The propagation characteristics of a uniform magneto-ionic duct of circular cross-section are determined for frequencies higher than the cyclotron frequency. The ratios (plasma wavelength)/(free space wavelength) and (power flowing in the plasma)/(power flowing outside) are evaluated and discussed as a function of the diameter/wavelength ratio and of the plasma permittivity for the propagation of circularly symmetrical modes. The Brillouin diagrams for frequencies higher and lower than the cyclotron frequency are also derived.

ASTIA NO.  
Contract No: AF 61 (052) - 145  
United States Air Force, Air Research and  
Development Command, European Office,  
Brussels, Belgium

Technical (Scientific) Note No. 2

TITLE: "PROPAGATION CHARACTERISTICS OF A MAGNETO-IONIC DUCT"

By: D. Formato and A. Gillardini

Date: 1 May, 1961

Pages: 39

Organization: SELENIA S.p.A., Via Tiburtina Km 12,400, Rome, Italy

ABSTRACT: The propagation characteristics of a uniform magneto-ionic duct of circular cross-section are determined for frequencies higher than the cyclotron frequency. The ratios (plasma wavelength)/(free space wavelength) and (power flowing in the plasma)/(power flowing outside) are evaluated and discussed as a function of the diameter/wavelength ratio and of the plasma permittivity for the propagation of circularly symmetrical modes. The Brillouin diagrams for frequencies higher and lower than the cyclotron frequency are also derived.

ASTIA NO.  
Contract No: AF 61 (052) - 145  
United States Air Force, Air Research and  
Development Command, European Office,  
Brussels, Belgium

Technical (Scientific) Note No. 2

TITLE: "PROPAGATION CHARACTERISTICS OF A MAGNETO-IONIC DUCT"

By: D. Formato and A. Gillardini

Date: 1 May, 1961

Pages: 39

Organization: SELENIA S.p.A., Via Tiburtina Km 12,400, Rome, Italy

ABSTRACT: The propagation characteristics of a uniform magneto-ionic duct of circular cross-section are determined for frequencies higher than the cyclotron frequency. The ratios (plasma wavelength)/(free space wavelength) and (power flowing in the plasma)/(power flowing outside) are evaluated and discussed as a function of the diameter/wavelength ratio and of the plasma permittivity for the propagation of circularly symmetrical modes. The Brillouin diagrams for frequencies higher and lower than the cyclotron frequency are also derived.

ASTIA NO.  
Contract No: AF 61 (052) - 145  
United States Air Force, Air Research and  
Development Command, European Office,  
Brussels, Belgium

Technical (Scientific) Note No. 2

TITLE: "PROPAGATION CHARACTERISTICS OF A MAGNETO-IONIC DUCT"

By: D. Formato and A. Gillardini

Date: 1 May, 1961

Pages: 39

Organization: SELENIA S.p.A., Via Tiburtina Km 12,400, Rome, Italy

ABSTRACT: The propagation characteristics of a uniform magneto-ionic duct of circular cross-section are determined for frequencies higher than the cyclotron frequency. The ratios (plasma wavelength)/(free space wavelength) and (power flowing in the plasma)/(power flowing outside) are evaluated and discussed as a function of the diameter/wavelength ratio and of the plasma permittivity for the propagation of circularly symmetrical modes. The Brillouin diagrams for frequencies higher and lower than the cyclotron frequency are also derived.